MXene Materials for Designing Advanced Separation Membranes

*Hüseyin Enis Karahan, Kunli Goh, Chuanfang (John) Zhang, Euntae Yang, Cansu Yıldırım, Chong Yang Chuah, M. Göktuğ Ahunbay, Jaewoo Lee, Ş. Birgül Tantekin-Ersolmaz, Yuan Chen, and Tae-Hyun Bae**

Dr. H. E. Karahan, Dr. K. Goh, Prof. E. Yang, Dr. C. Y. Chuah, Dr. J. Lee

Singapore Membrane Technology Center (SMTC), Nanyang Environment and Water Research Institute, Nanyang Technological University, Singapore 637141, Singapore

Dr. H. E. Karahan, Dr. C. Y. Chuah

School of Chemical and Biomedical Engineering, Nanyang Technological University, Singapore, 637459, Singapore

Dr. H. E. Karahan, Prof. Y. Chen

School of Chemical and Biomolecular Engineering, The University of Sydney, Sydney, New South Wales, 2006, Australia

Dr. C. J. Zhang

ETH Domain, Empa, Swiss Federal Laboratories for Materials Science and Technology, Überlandstrasse 129, CH-8600 Dübendorf, Switzerland

Prof. E. Yang

This is the author manuscript accepted for publication and has undergone full peer review but has not been through the copyediting, typesetting, pagination and proofreading process, which may lead to differences between this version and the Version of Record. Please cite this article as doi: 10.1002/adma.201906697.

Department of Marine Environmental Engineering, Gyeongsang National University, 38 Cheondaegukchi-gil, Tongyeong, Gyeongnam 53064, Republic of Korea

C. Yıldırım

Polymer Science and Technology Graduate Program, Istanbul Technical University, Istanbul 34469, Turkey

Prof. M. G. Ahunbay, Prof. Ş. B. Tantekin-Ersolmaz

Department of Chemical Engineering, Istanbul Technical University, Maslak, Istanbul 34469, Turkey

Prof. T.-H. Bae

Department of Chemical and Biomolecular Engineering, Korea Advanced Institute of Science and Technology, Daejeon 34141, Republic of Korea

E-mail: thbae@kaist.ac.kr

Keywords: 2D titanium carbides; Nanolaminates; Mixed-Matrix Composites; Nanocomposites; Molecular sieving

MXenes are emerging rapidly as a new family of multifunctional nanomaterials with prospective applications rivaling that of graphenes. This review aims to provide a timely account of the designing and performance evaluation of MXene-based membranes. First, the preparation and physicochemical characteristics of MXenes are outlined, with a focus on exfoliation, dispersion stability, and processability, which are crucial factors for membrane fabrication. Then, different formats of MXene-based membranes in the literature are introduced, comprising pristine or intercalated nanolaminates, and polymer-based nanocomposites. Next, the major membrane processes so far pursued by MXenes are evaluated, covering gas separation, wastewater treatment, desalination, and organic solvent purification. The potential utility of MXenes in phase inversion and interfacial polymerization, as well as layer-by-layer assembly for the preparation of nanocomposite membranes, are also critically discussed. Looking forward, exploiting the high electrical conductivity and catalytic activity of certain MXenes are put into perspective for niche applications that are not easily achievable by other nanomaterials. Furthermore, the benefits of simulation/modeling approaches for designing MXene-based membranes are exemplified. Overall, this review provides useful insights for materials science and membrane communities to navigate better while exploring the potential of MXenes for developing advanced separation membranes.

1. Introduction

Membrane design has long been a direct application area of nanomaterials research.[1–5] The exploitation of nanoparticles as fillers (nanofillers), yielding nanocomposite structures, for example, is a viable strategy of engineering the permeability, selectivity, and/or stability of polymeric/ceramic membranes. For selecting or producing the right fillers for the right membrane applications, numerous studies focused on the particle size/shape, pore size/shape, surface chemistry, and chemical stability of nanofillers as classical design parameters. Beyond, several nanomaterials also proved to be useful as supported nanolaminate membranes (NLMs), having asymmetric structures somewhat similar to thin-film composite (TFC) membranes. Among the nanomaterials used for membrane research, the graphene-family materials (GFMs) have attracted special and evergrowing attention.[6,7] GFMs have successfully served as functional fillers of nanocomposite membranes as well as NLMs with tunable nanochannels. Moreover, GFM-driven membrane research has revealed the unique advantages of flat materials in membrane development, providing crucial insights into the role of particle morphology and surface chemistry. Beyond GFMs, a wide range of two-dimensional (2D) inorganic, as well as organic nanomaterials, have been increasingly investigated for membrane applications.[8,9]

Among the 2D (nano)materials (2DMs) used in membrane research, exfoliated hexagonal boron nitrides (h-BNs), graphitic carbon nitride (g-C_3N_4) transition metal dichalcogenides (TMDs), and metal carbide, nitride, or carbonitrides (in short, MXenes) are of special interest as graphene analogs.[8,10] Owing to their strong structural, physical and/or chemical similarities, those materials are in an advantageous position for making full use of the lessons learned while developing GFM-based membranes. Besides, different 2DMs offer different material properties that might meet the needs of different applications. In this respect, MXenes are of particular interest due to their rich

surface chemistry and unique physicochemical properties. Albeit the majority of MXene literature is currently based on a specific type of MXene (i.e., $Ti_3C_2T_x$ – often derived from titanium aluminum carbide (Ti_3AlC_2) MAX phase), the MXenes are highly customizable as a family of materials.[11,12] The parent materials of MXenes, MAX phases, offer an immense compositional vastness with hundreds of known variations, and more than 30 varieties of MXenes reported to date.[11–16] The precursor selection not only determines the chemical but also affects the physical properties of resulting MXenes considerably. Besides, MXenes are post-functionalizable materials. During or after the etching-aided delamination/exfoliation of MAX phases, it is possible to introduce a variety of functional groups to MXenes, which provides another level of tunability.[17,18] Hence, MXenes constitute a highly versatile superfamily of nanomaterials and bring an unprecedented level of materials design capability at the disposal of advanced membrane research.

MXenes are arguably the fastest-growing 2DMs in the post-graphene era. Since their discovery in 2011,[19,20] they have attracted widespread research interest due to their intriguing electrical, thermal, mechanical, chemical, as well as biological properties.[21–24] As of January 1st of 2020, the unique term of "MXene" appears in the titles, abstracts, and/or keywords of >1500 publications cataloged in two major databases, with a clearly exponential expansion of the field as a function of published papers per year (**Figure 1**a). Naturally, a fine collection of reviews provided insights regarding their preparation, functionalization, purification, characterization, and materials properties.[25–31] Several reviews also focused on the application potential of MXenes for a wide range range of subjects including energy storage,[31–36] (electro)catalysis and sensing,[31,33,34,37] and biomedical,[38–40] to name a few. As separation membranes are closely related to thin films and composite materials, the discussions provided in some of those reviews hinted at the preparation of MXene-based membranes. However, only a couple of reviews[9,41–47] examined MXene-based separation membranes, albeit as a part of general discussions on the MXene applications or 2DM-

based membranes (see **Table S1**). Hence, no dedicated report has yet to discuss the current status and future prospects of MXene-based separation membranes in a dedicated manner. Given that ≈6% of MXene literature is already devoted to separation/purification applications (Figure 1b), which are mostly on membranes, we thought that it is timely to prepare this Progress Report focused on MXene-based membranes.

In this Progress Report, we aim to introduce the status and prospects of MXene-based membranes for high-performance separation/purification applications. To create a basis for discussion, we first introduce MXenes and MXene-based membranes, covering NLMs (a.k.a. laminar or lamellar membranes), mixed-matrix membranes (MMMs), and thin-film nanocomposites (TFNs). Next, we review the progress made in gas separation (including air filtering), water purification (i.e., solute rejection, bacteria removal, and desalination), and organic solvent purification (Figure 1c). Looking forward, we provide our future perspectives for MXene-based membranes, focusing strategically on four potential research directions: (1) Opening up niche membrane applications, (2) expanding to untapped membrane formats, (3) exploiting simulation/modeling approaches, and (4) scale-up efforts. Notably, given that the different application areas of MXenes are still hardly separable, we occasionally supplemented our discussions by borrowing findings made in other fields. Overall, we expect this review to provide stewardship and initiate new ideas for both materials science and membrane communities in expanding the scope and competitiveness of MXene-based research.

2. MXene-based Membrane Materials

We start the discussions by introducing the synthesis and properties of MXenes, emphasizing specific aspects directly relevant to the fabrication and separation/purification performance of resulting membranes. In addition, we briefly touch on certain critical notions regarding the design,

fabrication, and mass transport mechanisms of MXene-based membranes to create a springboard for in-depth discussions.

2.1. Preparation of MXene Nanosheets

The MXene materials are transition metal carbides, nitrides, and carbonitrides, with a general chemical formula of $M_{n+1}X_n$ (or $M_{n+1}X_nT_x$), where M, X, and T represent the early transition metals (e.g., Ti), carbon and/or nitrogen, and surface functionalities added through etching (e.g., −O, −F, or −OH), respectively.[12,19] There are two main ways of synthesizing MXenes: (1) Chemical vapor deposition (CVD) of molecular precursors (bottom-up approach), and (2) selective etching of parent materials (often MAX phases) followed by exfoliation (top-down approach). The CVD method can potentially produce high-quality 2D MXenes with large lateral size and few defects.[53] However, CVD is not practical for the fabrication of large-area membranes, and only a few types of carbide MXenes have been produced via CVD yet.[32] Thus, more emphasis is being placed on the top-down synthesis of MXenes currently.

The vast majority of the MXene-based membranes available in the literature are based on the top-down route, starting with MAX phases ($M_{n+1}AX_n$) as parent materials. MAX phase materials comprise of nearly closed-packed early transition metals (M) with the octahedral sites filled by C and/or N (X) atoms, giving rise to unexposed $M_{n+1}X_n$ layers (where n = 1, 2, or 3) stacked with layers of A-group elements (mostly groups 13 and 14) in an alternating multilayer fashion (**Figure 2**a).[32] Unlike graphite, where the graphene layers are held by weak intermolecular forces, the MAX phases are held by strong M−A metallic bonds, making their exfoliation by mere mechanical shearing very difficult.[25] To delaminate these layers, the idea is to capitalize on the relatively higher reactivity of M−A bond (compared to M−X bond), which is achieved by the selective removal of A atoms. Once the A-depleted $M_{n+1}AX_n$ stacks are formed ($M_{n+1}X_n$), exfoliation process becomes much easier,

resulting in exposed $M_{n+1}X_n$ nanosheets (MXenes for short). As the metallic M−A bonds are strong, the selective etching is commonly made by strong etchants under well-controlled conditions without drastically jeopardizing the 2D structure of remaining $M_{n+1}X_n$ stacks (Figure 2b). During the etching process, MXene nanosheets spontaneously form at a low concentration. However, the ultrasound-assisted exfoliation of $M_{n+1}X_n$ stacks,[56] which can be considered as multilayered MXenes, is the key step for obtaining MXenes at large quantities (Figure 2c). High-temperature treatment, on the other hand, favors the formation of 3D-like MXene networks.[32,33]

To date, over 150 different MAX phases have been synthesized based on 14 M and 16 A elements.[16] However, due to several factors including the relative ease of etching Al as A element, and the low cost (either purchasing or in-house synthesis) of Ti_3AlC_2, $Ti_3C_2T_x$ has served as the basis of MXene research to date.[12,32,57–60] The most commonly used etchant for MXene synthesis is aqueous hydrofluoric acid (HF). However, mainly due to the safety concerns associated with storing and handling of HF, there is a fast shift toward its in situ generation using hydrochloric acid (HCl) and a fluoride salt, such as lithium fluoride (LiF), ammonium hydrogen difluoride (NH_4HF_2), or ammonium fluoride (NH_4F).[32,61–65] As an added benefit, the cations (like Li^+) can intercalate between the $M_{n+1}X_n$ layers, which facilitate the exfoliation process by enlarging the interlayer spacings and weakening the interlayer interactions.[66–68] Irrespective of the use of HF directly or its generation in situ, the resulting MXene nanosheets end up with a general chemical formula of $M_{n+1}X_nT_x$, where T represents O, F, and/or OH as the terminating groups decorating the MXene surfaces after delamination.[32,69]

2.2. Properties of MXene Nanosheets

MXenes demonstrate several desirable properties that can be capitalized for designing high-performance membranes. Therefore, before introducing the membrane formats investigated so far, we highlight the properties of MXenes. We start with explaining the benefit of 2D morphology for

membrane design with examples from MXene literature. Given their direct relevance to membrane fabrication and stability, we later examine the solution processability and chemical stability of MXene dispersions in separate subsections. Then, we discuss the electrical, mechanical, and antimicrobial properties of MXenes due to their crucial roles in membrane performance for different applications.

2.2.1. 2D Morphology

Of particular importance is the 2D morphology of MXenes. Similar to the (2D) GFMs, the high-aspect-ratio of regular MXene nanosheets endows the resulting membranes with nanochannels that resulted in lengthened diffusion pathways for solute transport (**Figure 3**a). These nanochannels are formed by the pinholes, internal spacings between parallel and wrinkled nanosheets known as nanogalleries, and voids between the nanosheet edges which can be considered as nanoslits. The lengthening of the permeation pathways allows the differentiation of solute transport rates, which serves as the basis of selectivity for the membranes formed by MXenes (as with other 2DMs). In addition, by engineering the interlayer spacing of 2D MXene assemblies, one can create well-defined transport channels for enabling size-exclusion-based molecular separation (see Section 2.4). For example, $Ti_3C_2T_x$-based NLMs demonstrate an interlayer spacing of ≈0.64 nm in the wet state, which allows water transport but retains solutes of sizes larger than this interlayer spacing (such as methylene blue cations).[60] The interlayer spacing between the $Ti_3C_2T_x$ nanosheets can be decreased further to a range of 0.52 to 0.38 nm when dried and/or heated, making the resulting MXene-based membranes suitable for gas separation.[60,70] Apart from the interlayer spacing, the lateral dimension (flake size) of MXene nanosheets is also tailorable from 6 to <1 μm by varying the etching and exfoliation conditions.[71] In turn, it becomes possible to modulate the distance of the diffusion pathway, and together with tuning the membrane thickness, the separation performance of the

MXene-based membranes can be engineered.[71] Besides, as with other 2DMs, MXenes are not perfectly flat materials and can get wrinkled, which adds up to the microstructural properties of resulting NLMs (Figure 3b).

2.2.2. Solution Processability

Another important physicochemical property of MXene-based materials is their hydrophilicity, which is the main reason behind their good water processability. The inherent hydrophilicity of MXene-based materials stems from their surface terminal (functional) groups, which replace the A atoms in the MAX phase materials. These groups are typically based on oxygen and/or fluorine atoms. Notably, $Ti_3C_2T_x$ nanosheets exhibit a higher O/F ratio when synthesized using HCl-LiF solutions instead of 50% HF.[74] The higher O/F ratio, along with the presence of −OH functional groups and intercalating cations such as Li^+ and NH_4^+, can provide MXene nanosheets with a greater capacity to interact with water molecules. As a result, $Ti_3C_2T_x$-based NLMs exhibit high water wettability (high hydrophilicity) with water contact angles of ≈25–45°.[60,71] The presence of −OH functional groups and the associated negative charges (with high zeta potential values ranging between −30 to −80 mV) also opens up the possibility of surface modifications via chemical functionalizations and electrostatic attractions. To modify the surfaces of $Ti_3C_2T_x$ nanosheets, cationic surfactants or cationic/neutral polymers such as hexadecyltrimethylammonium bromide (CTAB), polyethyleneimine (PEI), poly(diallyldimethylammonium chloride) (PDDA), polydimethylsiloxane (PDMS), poly(ethylene oxide) (PEO), and poly(vinyl alcohol) (PVA) were utilized.[75–78] Beyond that, by leveraging silanol chemistry on −OH groups, the $Ti_3C_2T_x$ nanosheets were also grafted with organosiloxanes to give a multitude of functional groups including $-NH_2$, −COOR, $-C_6H_6$, and $-C_{12}H_{26}$.[79] These efforts not only confirm the feasibility of wettability tuning for MXene-based

materials but also demonstrate the chemical versatility of MXenes, which is desirable for membrane development.

2.2.3. Chemical Stability

Controlling the chemical stability of MXenes is crucial for both solution processability and the performance of resulting membranes. Under an inert gas environment, $Ti_3C_2T_x$ (T_x = F or OH) MXenes are fairly stable until 800 °C with a minimal level of oxidation (yielding anatase) at around 500 °C.[80] However, surface-exposed metal atoms of MXenes are more prone to oxidation, which might lead to spontaneous oxidation.[81] Keeping colloidal MXenes in argon-filled containers (at low temperatures) help preserve them for a longer period of time.[69] It is important to note that MXenes are also considerably more stable in the dry form (as films) and as embedded in a polymeric matrix (such as PVA).[69,82] On the other hand, the stability of MXenes (Ti_3C_2) can be dramatically improved by annealing under hydrogen atmosphere.[83]

2.2.4. Electrical Conductivity

The electrical conductivity of certain MXene-based materials is of particular interest to membrane applications. This is because certain MXenes (e.g., titanium carbide MXene) have probably one of the most attractive conductivities among all solution-processable 2DMs, including graphene.[32,68] Notably, $Ti_3C_2T_x$ films have a metallic conductivity as high as around 10000 $S \cdot cm^{-1}$, allowing them to demonstrate potential in modulating ions transport under an externally applied potential.[32,60,68] A pioneering study in the field has successfully attested this concept by modulating NaCl and $MgSO_4$ salts transport through a $Ti_3C_2T_x$ membrane via switching between positive and negative voltages.[84] They attributed this voltage gating effect to the change in electrostatic interactions between $Ti_3C_2T_x$ nanosheets and cations, which led to ions intercalation and corresponding alterations in the

interlayer spacing between $Ti_3C_2T_x$ nanosheets.[84] (For a detailed discussion on MXene-based electroresponsive membranes, see the Future Prospects section below.)

2.2.5. Mechanical Properties

The mechanical properties of MXene-based materials are also very interesting for membrane development. With its high Young's modulus at ≈0.33 TPa, single-layer $Ti_3C_2T_x$ MXene possesses an even higher elasticity than graphene oxide (GO), and other solution-processed 2DMs.[24] More importantly, when combined with polymeric materials such as PDMS or PVA, the $Ti_3C_2T_x$ nanosheets enhance the overall mechanical properties of the resulting nanocomposite films.[75,78] It is worth emphasizing that PDMS (hydrophobic) and PVA (hydrophilic) are common membrane materials with different wettability behaviors.

2.2.6. Antimicrobial Properties

In addition to the chemical and physical properties introduced above, the antimicrobial behavior of MXenes is also important for certain membrane applications. Colloidal dispersions of $Ti_3C_2T_x$ nanosheets exhibit strong antibacterial activity (against both Gram-negative and -positive bacteria), outpacing that of GO.[22] Importantly, potent antibacterial activity of MXenes is also revealed in surface-deposited or polymer-embedded forms as observed by different research groups.[85–87] (We will provide further evaluations on the antibacterial activity of MXenes below in Section 3.)

2.3. Fabrication of MXene Membranes

Here we focus on three types of membrane formats (Figure 3), which have been commonly utilized for preparing MXene-based membranes: (1) NLMs, (2) MMMs, and (3) TFNs. (Note that we provide further insights regarding the preparation of MXene-based membranes under the Future Prospects section.)

2.3.1. Nanolaminate Membranes

In academic research, the NLMs prepared by vacuum- or pressure-assisted filtration constitute the most extensively studied membrane format for MXene-based membranes (Figure 3a). To fabricate NLMs, the first step is to disperse MXenes in solvents (commonly water at an appropriate pH regime), forming a homogeneous and stable colloidal dispersion.[60,70,71,84,88,89] The lateral dimension of the flakes and choice of support membranes are the first two parameters of consideration for preparing such membranes. Besides, several parameters such as the concentration/volume of colloidal dispersions, as well as the pressure applied will directly impact the thickness, compactness, and integrity of the resulting membranes.[90,91] It should also be emphasized that there are alternative methods of preparing NLMs resembling the ones prepared by filtration methods. For example, Xu et al. has reported on the preparation a MXene membrane on flat-sheet polyacrylonitrile (PAN) supports via spin-coating. Likewise, dip-coating of MXene materials on a four-channel ceramic α-Al_2O_3 hollow fiber support was also demonstrated.[92]

Another key parameter in NLM fabrication lies in the solution processability of MXene-based materials, which in turn depends on the rheological properties of dispersions. It has been shown that the colloidal dispersions of $Ti_3C_2T_x$ may exhibit viscoelastic behaviors at different concentrations depending on the rate of exfoliation.[93] Specifically, single-layer $Ti_3C_2T_x$ dispersions reveal a noticeable viscoelastic behavior at a concentration as low as <0.36 mg·mL^{-1}, while multilayer $Ti_3C_2T_x$ dispersions can achieve high viscoelasticity with increasing elastic moduli at higher loadings.[93] These results demonstrate that the rheological versatility of $Ti_3C_2T_x$ dispersions is an important factor for membrane fabrications even beyond the preparation of NLMs. Apart from the ease of fabrication, NLMs also constitute a practical platform to showcase the effects brought by chemical functionalization and intercalation. To this end, PEI, borate ions, and silver (Ag), titania (TiO_2), and

ferric hydroxide ($Fe(OH)_3$) nanoparticles, as well as GO nanosheets had been employed to improve the performance of MXene-based NLMs.[70,71,86,93,94]

2.3.2. Mixed-Matrix Membranes

To our understanding, polymer-based MMMs and TFNs are still the more realistic membrane designs for practical applications. The concept of MMMs revolves around the goal of engineering the transport properties of membranes (continuous matrix phase) by the integration of filler particles (Figure 3c).[5] Fabrication of such membranes generally involves dispersing the filler material into the polymer dope solution before casting the membrane and inducing phase inversion either through solvent evaporation or nonsolvent-induced coagulation. A well-designed MMM should take into consideration the following: (1) Dispersion stability of the filler material in the organic solvent system adopted by the polymer dope solution, (2) uniformity and state of aggregation of the filler material in the as-prepared membrane, as well as (3) chemical compatibility of the filler material with the polymer matrix, especially at the filler/polymer interface.[5] In this regard, MXene-based materials are highly compelling given their hydrophilicity, polarity, and rich surface chemistry, which allow considerable versatility for further functionalization as well as strong interactions with a range of solvents. Notably, $Ti_3C_2T_x$ nanosheets are found to possess long-term dispersion and chemical stability in polar organic solvents such as *N*,*N*-dimethylformamide (DMF) and *N*-methyl-2-pyrrolidone (NMP), both of which are important solvents for MMM fabrications.[95] The presence of −OH terminations on $Ti_3C_2T_x$ nanosheets also offers the possibility of using classical silanol chemistry to functionalize the surface of the nanosheets and increase their chemical compatibility at the filler/polymer interfaces. Silanol chemistry is among the most extensively utilized chemistries for mitigating nonideal interfacial morphologies (essentially membrane defects).[5] Thus, successful

fabrication of $Ti_3C_2T_x$-based MMMs using various polymers (as matrix) had been reported for effective purification of water and organic solvents.[79,84,96,97]

The roles played by MXene fillers in the MMMs can range from leveraging the 2D morphology and narrow interlayer spacing for size exclusion, lengthening diffusion pathways for realizing selective solute transport, and tuning surface chemistries for promoting facilitated transport to altering the packing of polymer chains for enhancing mechanical properties and separation performances. In retrospect, these roles are not distinctly different from those played by other 2DM fillers (see ref. [5] for a general discussion of the roles of 2DMs as fillers). For MXene-based MMMs to truly add value to membrane-based separations, efforts should gear towards exploiting the unique advantages of MXene-based materials such as the high electrical conductivity (of certain MXenes). As an attestation to this proposal, a preliminary study had shown that a 1.5-µm-thick $Ti_3C_2T_x$/PVA MMM not only exhibited enhanced mechanical stability that was sufficiently robust to withstand repeated performance evaluations but also continued to stay electrically conductive, enabling water fluxes and electrostatically manipulated rejection rates to remain tunable by applying different voltages.[84]

2.3.3. Thin-Film Nanocomposites

Fundamentally speaking, the concept of TFN membrane is a modified version of TFCs, which combines the ideas behind MMMs and TFCs (Figure 3d and Figure 3e). Since the TFC membranes remain the most commercially successful membranes for wastewater treatment and desalination presently, TFNs are interesting for performance-driven research. Indeed, TFNs have demonstrated great promise for a wide range of applications including nanofiltration (NF), and osmotically driven processes including reverse osmosis (RO), forward osmosis (FO), and pressure-retarded osmosis (PRO). Similar to the conventional TFCs, the TFN membranes often comprise an ultrathin polyamide

(PA) selective layer over a porous substrate (support layer) to afford an asymmetric structure. And, the interfacial polymerization (IP) technique serves as the core method of preparing such membranes, which has not been systematically studied so far for MXene-filled membranes. (Since we regard IP as very promising method for developing MXene-based membranes, we further discuss its potential in the Future Prospects section below.)

2.4. Working Principles of MXene-based Membranes

Before evaluating the separation/purification performance, we would like to provide a light discussion on the separation mechanisms of MXenes-based membranes. In both MMMs and TFNs, MXenes serve as filler materials rather than directly acting as the selective component. Besides, as observed in many other filler materials,[5] the main contribution of MXenes in MMMs and TFNs is to engineer the transport properties of the matrix and lower the membrane resistance. Hence, we will focus on the separation mechanisms of NLMs, followed by a brief discussion on how MXenes improve the performance of MMMs and TFN membranes. (For more information on MMMs and TFNs, we recommend the readers to refer to ref.s [5,98–101].)

2.4.1. Gas Separation by Nanolaminates

One of the most common gas separation mechanisms of NLMs is Knudsen diffusion.[102] When the mean free path of a gas molecule is larger than the channel it travels, Knudsen diffusion acts as the dominant mechanism of transport.[103] Under such conditions, the molecular weights of the gases determine the separation selectivity. More precisely, the selectivity is inversely proportionate to the square root of the molecular weight of the permeating gas components as shown in Equation (1):[104]

$$J = \frac{\pi n r^2 D_k \Delta p}{RT d l} \quad \text{..... Eq. (1)}$$

where *J* is the flux of the membrane, *n* is the molar concentration of the gas, *r* is the pore radius, Δp is the transmembrane pressure, *R* is the gas constant, *T* is the temperature, τ is the tortuosity of the pores and *l* is the diffusion length. D_k is the Knudsen diffusion coefficient which is defined as given in Equation (2):

$$D_k = 0.66r\sqrt{\frac{8RT}{\pi M_w}} \quad \text{..... Eq. (2)}$$

where M_w is the molecular weight of the permeating gas.[105]

In addition, MXene-based nanolaminates have huge potential to separate via a facilitated (carrier mediated) transport mechanism. Facilitated transport is enabled by chemical carriers that can react reversibly with one gas component but not the other. This allows the interacting gas to permeate through the nanolaminate more preferentially than the noninteracting gas.[106] Owing to the rich surface chemistry and physicochemical versatility of MXene materials, MXene-based nanolaminates can be chemically modified with a multitude of different functional groups to target specific gas components in feed mixtures.

2.4.2. Liquid Separation by Nanolaminates

Nanolaminates for water and organic solvent purification typically separate via two main mechanisms: (1) Size exclusion, or (2) Donnan exclusion principle.[94] As discussed in Section 2.2, the size of the interlayer spacing plays an instrumental role in the size exclusion mechanism. Solutes which are larger than the interlayer spacing between MXene nanosheets are sieved out or rejected, while smaller solutes are allowed to permeate through the interlayer spacing (Figure 3a).[105,107] Also, given that MXene nanosheets are highly negatively charged (see Section 2.2), charged solutes, such as ions, polyelectrolytes and organic dyes, can be separated via the Donnan exclusion principle. In Donnan exclusion principle, co-ions, with the same charge as the membrane, are electrostatically

repelled away from the membrane, which, in turn, drives the rejection of the counter-ions to maintain electroneutrality of the solution.[108] Because of this electrostatic repulsion of charged solutes, the nanoslits and interlayer spacing of these nanolaminates can be larger than the size of the solutes to be separated. The interlayer spacing of MXene-based nanolaminates is typically controlled in the nanometer to subnanometer regime. Thus, the NF process is best suited for nanolaminates for water and organic solvent purification. The flux of the solvent permeating through the MXene-based NLMs can be defined by Hagen-Poiseuille equation, Equation (3), which is valid for NLMs of other 2DMs:[109]

$$Flux = \frac{h^4 \Delta p}{12 L^2 \eta \Delta x} \quad \text{..... Eq. (3)}$$

where h is the d-spacing between the MXene nanosheets, Δp is the transmembrane pressure, L is the average lateral dimension of the MXene nanosheets, η is the viscosity of the solvent, and Δx is the membrane thickness.

2.4.3. Separation by Composite Membranes

Contrary to the NLMs, MXenes do not have a direct influence on the separation mechanism of MMMs and TFN membranes. This is because their main objective is to serve the role of filler materials for lowering mass transfer resistance and achieving performance enhancements. Hence, adding MXenes does not alter the separation mechanism that is already governing the transport behavior of the membranes. For example, MMMs (for gas separation and pervaporation) and the "skin-like" selective layers of TFN membranes (for NF, and RO applications) possess nonporous (dense) structures where solutes permeate via a solution-diffusion mechanism. According to the solution-diffusion mechanism, solute permeability is a function of its solubility and diffusivity as shown below in Equation (4).

$$P = S \cdot D$$ ..... Eq. (4)

where *P* is the permeability of the membrane, *S* is the solubility and *D* is the diffusivity of the solute permeating through the membrane.[5]

Solubility is a thermodynamic term which quantifies the amount of solutes sorbed by the membrane, while diffusivity is a kinetic term which accounts for how fast the solute diffuse through the membrane.[104] When MXene fillers are incorporated into the polymer matrix of MMMs or the selective layer of TFN membranes, the nanochannels made up by the interlayer spacing of layered MXenes and the nanogaps at the polymer/filler interface can provide supplementary pathways of lower transport resistance as compared to the dense polymer matrix (Figure 3c to Figure 3e). This increases the diffusivity of the solutes, leading to an enhancement in solute permeability. Similar enhancement in solute permeability can also be achieved by incorporating chemically functionalized MXenes with enhanced affinity towards the solutes to strengthen the solubility of the solutes. Hence, in the case of dense membrane structures, solute transport remains hinged on the solution-diffusion mechanism and the addition of MXene fillers can alter diffusivity and solubility of solutes to bring about an engineering of the transport properties of the membranes.

3. MXene-based Separation Membranes

MXenes offer interesting materials properties that are well-aligned with the efforts aimed at realizing next-generation membranes. As introduced above, MXenes are also suitable for designing different types of membranes. Accordingly, MXenes have been so far utilized for a wide range of separation/purification membrane applications (Table S2). Below, we discuss the progress made in MXene-based according to gas, water, and organic solvent separation/purification applications below.

3.1. Gas Separation

Despite being in its infancy stage, MXenes have already demonstrated great promise in membrane-based gas separation. Ding and co-workers[89] fabricated MXene-based NLMs via vacuum-assisted filtration on anodic aluminum oxide (AAO) supports. By simply peeling off the deposited film, the researchers could prepare "freestanding" MXene membranes showing high mechanical robustness (**Figure 4**a and Figure 4b). Gas permeation analysis revealed that the freestanding MXene nanolaminates are highly permeable to small gas molecules (He: 2164 barrer; H_2: 2402 barrer) at 25 °C and 1 bar. As the permeation of larger gas molecules, including CO_2, O_2, N_2, and CH_4, were quite low, the authors could demonstrate high selectivity for several small/large gas pairs. For example, H_2/CO_2 gas pair reached a high ideal and mixed-gas selectivities of 238.4 and 166.6, respectively, despite a selectivity of only ≈4.7 was predicted based on Knudsen diffusion. As a result, the demonstrated membrane exceeded the 2008 Robeson Upper Bound[103] (a hypothetical boundary line that showcases a practical performance limit of conventional polymeric membranes) significantly (Figure 4c). On the other hand, the ideal CO_2/N_2 selectivity was very low since the permeability of CO_2 was lower than that of N_2 (CO_2: 10 barrer; N_2: 19 barrer). The authors attributed this observation to the restriction of CO_2 diffusion due to strong interaction of CO_2 molecules and MXenes. Considering that MXenes are rich in oxygen-containing functional groups, they might be exerting a "trapping effect" on the permeating CO_2 molecules. The authors have verified this argument by checking the interaction energies of CO_2 and N_2 with MXenes, which were −175.1 and −97.5 kJ·mol^{-1}, respectively. Therefore, MXene NLMs appear promising for applications that require the suppression of CO_2 permeation.[89]

One strategy to increase the CO_2 permeation is to reduce the overall transport resistance by developing thinner NLMs with well-tuned interlayer spacings. Shen et al.[70] had successfully employed this strategy by manipulating the crosslinking of MXene nanosheets with borate ($B_4O_7^{-2}$) and PEI (Figure 4d and Figure 4e). They demonstrated that both borate and borate/PEI intercalation

allowed the discrimination between CO_2 and CH_4 (or N_2) together with an increase in mechanical strength. This was further verified with a 43% increase in the equilibrium CO_2 adsorption of borate/PEI-intercalated MXene (13% for borate-modified MXene) as compared to the pristine MXene (Figure 4f). As a result, the borate/PEI-intercalated MXene-based membranes transcended the separation performance of even MOF-based membranes (Figure 4g). On another aspect, it had been reported that the composition of the feed gas (i.e., relative humidity) substantially affect the overall gas separation performance of MXene-based membranes. Such an effect had been verified by Shen et al.,[70] where the H_2/CO_2 selectivity plummeted for about 50% (from 19.7 to 9.8) as the relative humidity increased from 40% to 90%. The widely accepted explanation for such an observation is the facilitated transport of CO_2 by H_2O molecules that are intercalated between the nanogalleries. Thus, considering the fact that moisture is typically present in the feed streams for CO_2-based separation processes,[110–112] it might be beneficial to carry out a pre-treatment to dry feed gas streams in future studies.

In addition to room-temperature operations, MXenes are also useful for niche gas separation applications at high temperatures. Fan et al.[113] have shown that MXene-based NLMs give a high selectivity of 41 for H_2/N_2 separation at 320 °C. Plus, their AAO-supported MXene membrane showed no sign of degradation up to 200 hours of operation.[113] We find this observation promising for industrially relevant H_2 separation operations. In another promising demonstration, Liu et al. employed MXenes as the filler of a poly(ether-block-amide) (PEBA) MMM for CO_2 capture.[73] Using $Ti_3C_2T_x$ nanosheets at a filler loading as low as 0.15 wt%, the researchers have prepared high-performance composite membranes on PAN supports by spin-coating. Owing to the preferential affinity of (polar) CO_2 to (polar) $Ti_3C_2T_x$ particles and PEO blocks in PEBA used, the resulting MMM reached a remarkable CO_2/N_2 selectivity of 72.5 with the CO_2 permeance of 21.6 GPU. Importantly, the resulting membrane also showed good stability in a 120-h-long continuous

operation.[73] Again, using two PEBA varieties (and a water soluble polyurethane), Shamsabadi et al.[114] also recently developed MMMs for CO_2 capture. With Pebax® 1657, which contains PEO blocks, they have shown high selectivity and permeability, well exceeding the 2008 Robeson upper bound for CO_2/N_2. Importantly, they also observed that while the $Ti_3C_2T_x$ nanosheets exposed to open air degrades fast, MMMs are stable for 6 months as the polymer matrix serves as a protective layer.[114]

On a different note, although technically not a gas separation application, we think it is relevant to introduce here a recent study concerning the filtration of fine particulate matter (PM2.5: atmospheric particles with an effective aerodynamic diameter below 2.5 μm) from air using MXene-incorporated PAN-based filters.[87] As considered in the very concept of effective aerodynamic diameter, the performance of particulate air filters is influenced not only by the mesh size of filters but also the attraction of particles to the filter surfaces.[115] Accordingly, the authors added just 0.005 to 0.080 wt% of MXene into PAN (by combining MXene and PAN as the electrospinning precursor). The resulting electrospun composite filter exhibited superior PM2.5 removal performance in terms of both filtering capacity (>2 times) and rate (4.2 vs. 44 $\mu g \cdot cm^{-2} \cdot h^{-1}$). Besides, using a model Gram-positive species (*Staphylococcus aureus*), they have reported some preliminary observations on the inhibition of bacterial growth on the composite filters developed.[87]

3.2. Water Purification

For fabricating NLMs for gas separation, one of the most sought material properties of MXenes is likely their 2D morphology, which is manifested by all 2DMs. For developing water separation membranes, on the other hand, MXenes offer much more. High surface charge, hydrophilicity, ion adsorption capacity, electrical conductivity, mechanical robustness, chemical tuneability, photocatalytic and photothermal, as well as antibacterial properties are among the most attractive

attributes of MXenes for water separation. Accordingly, MXene-based membranes have been tested by many research groups for a wide range of water purification applications. We subdivide this literature into two major topics: (1) Wastewater treatment, and (2) water desalination. For wastewater treatment, we mainly examine the studies focused on solute removal and bacterial disinfection. For water desalination, we cover molecular sieving, as well as photothermal membrane distillation.

3.2.1. Wastewater Treatment

Aiming at applications in wastewater treatment, Ding et al.[71] assembled $Ti_3C_2T_x$ MXene nanolaminates on AAO support via vacuum-assisted filtration. To create abundant channels that facilitate water transport, they have utilized MXenes with lateral sizes of ≈100–400 nm. As an additional strategy, they have intercalated MXenes with positively charged $Fe(OH)_3$ nanoparticles, which were later removed during the membrane fabrication, leaving a larger interlayer spacing between the MXene nanosheets (**Figure 5**a to Figure 5c). As a result of this combined strategy, an extraordinarily high water permeability of >1000 $L{\cdot}m^{-2}{\cdot}h^{-1}{\cdot}bar^{-1}$ ($LMH{\cdot}bar^{-1}$) was achieved (Figure 5d). Plus, their MXene membrane retained a rejection efficiency of >90% for organic molecules having average molecular sizes above 2.5 nm. To enable the rejection of small dye molecules (with hydrated diameters in the range of 1.0–1.6 nm), Kang et al.[94] later incorporated 10–30 wt% GO nanosheets into MXene nanolaminates (Figure 5e). While the thickness of individual hydroxylated MXene nanosheets was ≈0.92 nm, the hydrated interlayer spacing of hybrid nanolaminate was larger at ≈1.43 nm. Thus, the effective nanochannel size of the hydrated MXene-GO composite membranes was ≈0.5 nm (due to stacking effect). During the pressure-driven filtration test, the MXene-GO composite membranes exhibited high rejection rates for charged dye molecules with a hydrated radius of >0.5 nm but performed worse for neutral and smaller dye molecules (Figure 5f). This

observation indicates that the nanogalleries formed in MXene nanolaminates provide size exclusion effect, and the (negative) surface charge enhances the rejection of (charged) dyes by electrostatic repulsion.[94]

Wang et al. have employed double-layered MXene nanosheets for the preparation of supported membranes by vacuum-assisted filtration.[109] Their membranes possessed rigid and highly ordered nanochannels, providing fast water transport exceeding a water permeability of 2,300 LMH·bar^{-1} (Figure 5g).[109] More recently, by again combining MXenes and GO, Liu et al.[116] have reported hybrid NLMs exhibiting higher rejection rates for organic dyes They have shown the rejection of humic acid as well as bovine serum albumin.[116] Nevertheless, it should be kept in mind that MXene-GO hybrids exhibit lower water permeance than pure MXene NLMs, in general. We mainly attribute this general observation to the role of lateral size differences of MXene and GO nanosheets used in these studies. Therefore, there is a need to pursue more systematic investigations.

In another interesting work, researchers have prepared MXene-incorporated mesoporous TiO_2 membranes and tested them for dextran rejection (Figure 5h).[92] Importantly, they used 1.0 wt% MXene nanosheets only. They coated disc-shaped and hollow fiber α-Al_2O_3 supports with MXene dispersion by spin-coating and dip-coating, respectively. After drying, they calcined the hybrid membranes composed of TiO_2 hydrosols and MXenes, at 400 °C and obtained a durable membrane, which showed superior dextran rejections. The authors attributed the enhanced performance of TiO_2-MXene membranes to the prevention of structural defects by MXenes. It was likely that MXenes limited the infiltration of hydrosol particles through the support during membrane fabrication and sealed large defects, providing better dextran rejection without sacrificing the water flux dramatically.[92] In a related work, Sun et al. later varied different parameters, such as the

loading ratio of MXenes, dip-coating duration, and the duration and temperature of the calcination process.[117] For 1 wt% and 5 wt% MXene incorporations, they observed only <20% and <40% decline in water flux, respectively. Notably, they could manipulate the molecular cut-off and pore size of TiO_2-MXene membranes by playing with the rest of the parameters effectively.[117]

When it comes to the practicality of water treatment membranes, the resistance of membranes to fouling is equally critical. On many occasions, a fast-fouling membrane has a limited chance for practical applications, if any. In this regard, the MXenes appear promising as a new material platform. Rasool et al.[85] demonstrated that the MXene NLMs can effectively inhibit the growth of both Gram-positive and -negative bacteria (**Figure 6**a). Interestingly, they also observed that the MXene membranes exhibit higher antibacterial activity when oxidized in open-air naturally (Figure 6b). Later, Pandey and coworkers have shown a high-performance composite NLM composed of silver nanoparticles (AgNPs) and MXenes (Figure 6c).[86] By adding 21% AgNPs, they significantly improved the antibacterial activity of MXene membranes. Presumably due to the synergistic antibacterial activity of AgNPs and MXenes, hybrid AgNP-MXene membranes (Ag@MXene) showed virtually complete inhibition of *Escherichia coli* (*E. coli*) cells (Figure 6d). And, the bacterial cells grown on Ag@MXene membranes lost their envelope integrity considerably (compare Figure 6e and Figure 6f). Importantly, the inclusion of AgNPs also improved the water permeance (Figure 6g), while no significant drop occurred in the rejection of Rhodamine B, methyl green, and BSA (Figure 6h).[118] In addition to biofouling, separation membranes also suffer from the fouling of oily substances, particularly for wastewater treatment processes. Oil-water separation is an important subject on its own. To this end, Saththasivam et al.[119] and Li et al.[120] had reported on oil-water separating nanolaminates by depositing MXenes on print paper and polyethersulfone (PESf) substrates, respectively. Both studies showed promising oil-water separation results with low fouling

and high resistance to oils (including oily solvents).[119,120] (Further discussions on the solvent resistance of MXene-based membranes are available below in Solvent Purification section.)

3.2.2. Water Desalination

Under the pressing need to increase the efficiency of desalination processes, nano-enabled ion sieving membranes have gained ever-increasing attention in the last couple of years. The basic idea behind ion sieving membranes is mainly size exclusion and Donnan exclusion principles. For MXene-based NLMs, the most practical way to achieve this is to engineer the interlayer spacing for excluding hydrated ions while allowing water molecules to pass through. To this end, several studies have evaluated the ion (and water) transport through MXene-based membranes. Ren et al.[60] compared the water and positively-charged ions transport behavior of $Ti_3C_2T_x$ MXene- and GO-based NLMs. They observed that a 1.5-µm-thick MXene nanolaminate (**Figure 7**a and Figure 7b) provided around 6 times higher water permeability than a GO membrane of comparable thicknesses (37.4 vs. 6.5 LMH·bar^{-1}). The average nanochannel size of the MXene nanolaminates was around 0.64 nm, which allowed the transport of around three layers of water molecules. Accordingly, this thick MXene membrane could reject any ions with a hydration radius of larger than 0.64 nm, but ions with a hydration radius smaller than 0.64 nm permeate through. The charge of ions also plays a critical role in MXene nanolaminates. Due to the strong negative charge of MXenes, multivalent cations (e.g., Mg^{2+}, Ca^{2+}, and Al^{3+}) have shown slower permeation rates than monovalent ones given that their high charges have the capacity to narrow nanochannels in the MXene nanolaminates via electrostatic attraction (Figure 7c). On the other hand, small-sized monovalent cations such as Na^{+} can expand nanochannels by forming an electric double-layer (Figure 7d). The results by Han and coworkers supported these conclusions.[121] In their experiment conducted using MXene nanolaminates supported with PESf ultrafiltration membranes, they observed a 23% rejection for

Mg^{2+} ($MgCl_2$) while Na^+ rejection remained at 13.8% (NaCl) despite a slightly higher flux achieved for $MgCl_2$ solution (460 LMH) than for NaCl solution (435 LMH).

In their comprehensive study, Kang et al.[94] also investigated the transport of salt ions across the MXene-GO composite membranes (Figure 5e). Nevertheless, their MXene-GO nanolaminate composite membranes recorded a poor ion rejection of below 11% for both NaCl and $MgCl_2$ under pressure-driven conditions. Similar to the pure MXene and GO nanolaminates, the nanochannels of hydrated MXene-GO hybrid membranes were too large to exclude small ions with hydrated diameters less than 0.5 nm.[122] To address this issue, Sun et al. explored the utility of sintering temperature (60, 200, 300, 400, 450, 500 °C) on engineering the interlayer spacing of MXene ($Ti_3C_2T_x$) layers coated on tubular α-Al_2O_3 substrates.[123] MXene membranes dried at 60 °C had an interlayer spacing of 3.71 Å, which dropped to 2.68 Å at 400 °C sintering. When the sintering temperature was 450 °C and above (in air), partial oxidation of the MXene layer was observed as manifested by the color change of the membranes (from dark green/gray to reflective white). Importantly, the sintering of MXenes membranes at 400 °C gave the best rejection rates for all salts tested (Na_2SO_4, $MgSO_4$, NaCl, and $MgCl_2$).[123] Collectively, all these studies show that the interlayer spacing of MXene nanolaminates is the key for desalination applications. Thus, the importance of preventing the swelling of MXenes during operation becomes clearer. Lu et al. very recently proposed a strategy to address this issue.[124] By temperature-induced self-crosslinking of hydroxylated $Ti_3C_2T_x$ (via H_2O condensation), they managed to develop anti-swelling membranes. As expected, the salt rejection performances of the membranes improved as the degree of crosslinking increase but at the expense of decrease in permeability.[124] Further reducing the thickness of such membranes might be promising for a wide range of applications.

2DMs, including MXenes, offer desirable ways of supplying freshwater out of seawater owing to their photothermal properties. The conversion of the sunlight (solar) energy into heat is useful for evaporating water, giving rise to solar distillation. To extend this concept, it is possible to combine the idea of solar distillation with membrane technologies, yielding photothermal membrane desalination/distillation. Wang et al. made the first demonstration of MXenes' (Ti_3C_2) utility for photothermal desalination, with an extraordinarily high light-to-heat conversion efficiency.[125] By depositing MXenes on polyvinylidene difluoride (PVDF) supports and surface modifying with PDMS, Wang et al. achieved a membrane that could self-float on the water surface. Using this membrane platform, they could achieve ≈84% conversion efficiency under one sun irradiation with a pretty fast heating rate (Figure 7e).[125] In a subsequent study, Que and coworkers[126] have prepared a similar self-floating membrane by modifying the MXene layer deposited on PVDF with a fluorinated silane coupling agent, trimethoxy(1H,1H,2H,2H-per-fluorodecyl)silane. Owing to the antiwetting behavior of the surface modifying agent, the resulting membrane could handle real seawater (that contains organics and heavy metals) without the accumulation of salt crystals on top of the membrane (Figure 7g to Figure 7j). Hence, they could achieve an energy conversion (solar to steam) efficiency of 71% with a high level of stability (>200 h operation). Most importantly, the hydrophobic MXene membrane showed a remarkable desalination performance for different cations (Figure 7k).[126] Going further, Tan et al. have tested the feasibility of direct contact membrane distillation with MXene-incorporated membranes.[127] Similar to the material designs demonstrated in self-floating membranes, they coated the MXene-deposited PVDF supports with PDMS. Moreover, using these hydrophobic membranes, they reached a photothermal conversion of 5.8 $kW \cdot m^{-2}$ in a solar-assisted membrane distillation. They also showed the antifouling properties of their membranes with feeds containing 200 ppm of bovine serum albumin and 10 $g \cdot L^{-1}$ of NaCl (Figure 7l).[127] Going one step further, Zha et al.[128] reported on

antibiofouling filters for photothermal distillation prepared by dip-coating highly porous cellulose supports (pore size: 30–50 μm) with $Ti_3C_2T_x$. As an important point, $Ti_3C_2T_x$-based filters exhibited superior performance for steam generation and bacterial disinfection compared to GO-coated filters.[128]

3.3. Organic Solvent Purification

Owing to their high solvent resistance, MXenes are promising for the purification of organic solvents.[75,79,109] With their elastic moduli at around 260–440 GPa, which is comparable to that of GO (≈110–420 GPa), MXenes are useful for obtaining highly robust membranes.[25,129] In addition, it is possible to limit the solvent uptake and swelling of MXene-filled membranes for different solvents by functionalization. For example, $Ti_3C_2T_x$-NH_2 and $Ti_3C_2T_x$-COOR derivatives have inhibited solvent uptake and swelling (of PEI- and PDMS-based membranes) more efficiently against nonpolar solvents (e.g., toluene or n-heptane), while alkyl-modified derivatives ($Ti_3C_2T_x$-C_6H_6 and $Ti_3C_2T_x$-$C_{12}H_{26}$) performed better with polar solvents (e.g., isopropanol or ethyl acetate).[79] As such, MXenes attracted growing attention for organic solvent nanofiltration (OSN) as well as pervaporation of solvent mixtures, both of which demand highly stable membranes under long-term exposure to organic solvents.

3.3.1 Organic Solvent Nanofiltration

In a pioneering study, Wu et al. prepared PAN-supported TFN membranes by incorporating different amounts of hydroxyl-rich $Ti_3C_2T_x$ into PEI or PDMS matrix (**Figure 8**a).[75] Irrespective of the loading ratio of MXenes and the type of polymer matrix, all membranes provided superior rejection to oligomeric (200 to 1000 Da) polyethylene glycol (PEG) molecules in isopropanol (Figure 8b and Figure 8c). Notably, PAN/PEI-$Ti_3C_2T_x$-4 (with 4 wt% MXene loading) exhibited ≈99.4% rejection to PEG-800 (at 10 bar).[75] To explore the role of chemical functionalization of MXenes on PEG rejection,

Hao *et al.*[79] have adopted a very similar approach. By fixing the ratio of MXene loading at 3 wt%, they found that different functionalities are useful for different solvents.[79] As hinted in the previous paragraph, the swelling/uptake behavior of resulting membranes is critical for this outcome.

As an alternative method, Han et al. have prepared MMMs by incorporating $Ti_3C_2T_x$ into a polyimide (P84®) matrix via phase inversion (PI) followed by crosslinking with triethylenetetramine (TETA).[133] By optimizing the filling ratio, they achieved a virtually complete rejection of gentian violet (a.k.a. crystal violet, 408 $g \cdot mol^{-1}$) at a high flux (268 $L \cdot m^{-2} \cdot h^{-1}$) under 0.1 MPa and ambient temperature. Their membrane also showed an excellent solvent resistance to dimethylformamide (DMF), acetone, and methanol after crosslinking.[133] As we have pointed out above for dye removal from aqueous samples, MXene-based NLMs are also useful for rejecting dyes from organic solvents. With their Nylon-supported MXene-only nanolaminate, Wang et al. achieved a rejection rate of over 96% for the organic dye molecules larger than >2.0 nm from isopropanol (Figure 8d).[109] More recently, Wei et al.[130] reported a Nylon-supported GO/MXene hybrid NLM that can also reach over 90% dye rejection rates (Figure 8e). While testing their membranes with different organic solvents (i.e., acetone, methanol, ethanol, and isopropanol), they also demonstrated the high stability of hybrid MXene-GO NLMs for long-term operations.[130]

The flux of MXene-based OSN membrane is also worth noting, considering that it depends on the type of solvents used. It is well-established that the flux of incompressible and Newtonian fluids passing through channels made up of 2DMs can be described well by Hagen-Poiseuille law, Equation (3). The utility of Hagen-Poiseuille law for MXene-based membranes have been shown by Wang et al.[109] and Wu et al.[18] for NLMs, and Wei et al.[130] for TFNs. In accordance, the permeance values obtained in both cases were inversely proportionate to the viscosity of the organic solvents tested. Wang et al.[109] also demonstrated that the permeance through nanolaminates showed a

further inversely proportionate relationship to both molecular diameter and solubility parameter of the organic solvents. This suggests that the geometry as well as physicochemical nature of the nanochannels formed in MXene-based NLMs directly influence the permeation behavior of solvents during OSN process.

3.3.2. Solvent Dehydration by Pervaporation

In addition to OSN, MXene-based membranes have been effectively employed for the pervaporation-based dehydration of various solvents by different groups.[96,131,132] Similar to OSN membranes, organic solvent pervaporation membranes should also be stable under long-term exposure to organic solvents. Xu et al. have prepared such a stable MMM composed of chitosan and 1–5 wt% $Ti_3C_2T_x$. For ethanol dehydration, chitosan-MXene MMM with 3 wt% loading remarkably exhibited high improvement in both flux and separation factor by almost 25% and 250%, respectively (Figure 8f). They have also tested the role of operation temperature for dehydration of ethyl acetate and found 50 °C as an optimum value (Figure 8g). As is known, higher temperatures increase the swelling and hence free volume of such membranes, causing high flux at the expense of lowered selectivity.[96] In another very recent report,[131] Liu et al. prepared a PAN-supported TFN membrane by incorporating MXenes into (hyperbranched) PEI based on a membrane design approach similar to two earlier studies.[75,79] (In view of their link to IP chemistry, we will further discuss these three studies in the Future Prospects section.) With their highly uniform PAN/PEI-Ti_2CT_x membranes, Liu et al. could reduce the water content in the isopropanol/water mixture from 10 to <1 wt% with a flux (at 50 °C) that outperformed various types of membranes available in the literature (Figure 8h). However, they found that $Ti_3C_2T_x$ provides inferior results in terms of selectivity, which might be due to their lower hydrophilicity or higher layer thickness.[131] In another recent work, Wu et al. demonstrated the utility of Nylon-supported $Ti_3C_2T_x$ membranes for the

dehydration of alcohols. Their 2 μm-thick MXene membranes did not provide very high fluxes or separation factors (Figure 8i). However, their membrane provided quite an appealing performance at room temperature compared to 50 °C, with more than 30% higher separation factor at only ≈10% lower flux. Besides, they did not observe a serious deterioration in long-term performance, albeit with noticeable fluctuations of both flux and selectivity (Figure 8i).[131]

4. Future Prospects

The literature on MXene-based membranes are growing very fast particularly in the last two years. However, we believe most of this progress is based on the applications that can also be met by GFMs or some other 2DMs (depending on the cases). Besides, the majority of published studies are on NLMs prepared by vacuum-filtration of MXenes only. Given these general observations, we think it would be more effective to conduct research in the following directions: (1) Focusing on applications that MXenes can offer more than other 2DMs, and (2) exploring MXene-polymer composites in depth by visiting more established and scalable methodologies used in designing polymer-based separation membranes. Going further, we believe simulation/modeling techniques might help identify the areas and membrane designs in which MXenes might show superior performance. To this end, we formulated a four-legged Future Prospects as follows: (1) Promising membrane operations, (2) underutilized membrane formats, (3) simulation/modeling approaches, and (4) scale-up efforts.

4.1. Promising Membrane Operations

4.1.1. Electroresponsive Membranes

Previous studies on various material systems have shown that electroresponsive membranes are promising for water treatment applications.[134–136] Given the outstanding electrical, electrochemical,

and mechanical characteristics, MXenes are promising for designing electroresponsive membranes. Recently, Ren et al. have reported the utility of MXenes for fabricating electroresponsive membranes in their pioneering study.[84] They first deposited MXene-based NLMs ($Ti_3C_3T_x$) on PVDF supports with vacuum-assisted filtration. Then, by modulating the external voltage applied, they tuned the interlayer spacing (as well as surface charge) of the MXene nanolaminates for improved rejection towards metal ions and a charged organic dye (**Figure 9**a). They found that, under an osmotically driven condition (i.e., concentration gradient), a negative potential (−0.6 V) restrains the permeation of both monovalent (Na^+, NaCl) and divalent (Mg^{2+}, $MgCl_2$) cations through the MXene membranes. (And, a positive potential, +0.4 V, increases the permeation rates of ions.) Besides, under vacuum, they could improve the rejection rate of a positively charged dye (methylene blue) by applying a negative potential to MXene membrane (Figure 9b). Further, they have also demonstrated that larger MXenes flakes (prepared via a less intense exfoliation method) provide better electrical conductivity and mechanical stability, leading an improved performance for solute rejection.[84] As further studies, it would be interesting to address the deterioration of the electroresponsive performance of such MXene-based NLMs upon repeated cycles of use. It is necessary to elucidate the nature of electrochemical reactions taking place during such operations, in more detail. Indeed, there is a growing fundamental interest to better control the electrochemical behavior of MXenes to exploit them as electrocatalsyts for a wide range of applications.[33,137,138] Reaching a better understanding of the interactions between ions and MXenes on top of this will broaden the horizons of MXenes-based membranes for application scenarios beyond separations. Among those application areas, we may consider (membrane) capacitive deionization,[139] light-controlled nanofluidics,[140] osmotic energy harvesting,[141] (membrane) fuel cells,[142–145] and lithium-sulfur batteries,[146–148] to name a few. Reciprocally, the progress to be made in these areas might help accelerate the development of MXene-based membranes for separation applications. Thus, we

recommend researchers to consider these applications enabled by MXenes (and other 2DMs) with a more holistic approach through the lens of nanoionics.[149]

4.1.2. Reactive Membranes

Nanomaterial-enabled reactive membranes provide attractive means of wastewater treatment based on the in-situ removal of organic or ionic contaminants, commonly via reductive and/or oxidative reactions.[150–152] Unlike the inert ones, the reactive membranes might help avoid the need for additional steps of separation processes or the consumption of expensive chemicals. However, the catalytic performance of the nanomaterials should be high and long-lasting. Pandey and co-workers[153] have recently demonstrated high-performance reactive membranes capable of converting carcinogenic bromate (BrO_3^-) ions into less toxic bromide (Br^-) ions. Without the use of an additional catalyst or energy input, they have achieved an astonishing reduction capacity of 321.8 mg BrO_3^- per gram of $Ti_3C_2T_x$ with a virtually complete reduction (at pH 7). And, in the presence of co-ions such as SO_4^{2-}, NO_3^-, and PO_4^{3-}, the conversion rate showed a minor drop to ≈92% only. One drawback of the demonstrated system was the partial oxidization of MXene ($Ti_3C_2T_x$), which limits its reusability as a reactive membrane. Therefore, it is imperative to enhance the stability of MXenes for long-term performance.[153] As another future direction, it is essential to target applications beyond the detoxification of bromate. Ying et al.[154] previously showed that $Ti_3C_2T_x$ nanosheets exhibit a unique reductive removal performance for the conversion of toxic chromium(IV) ions (Cr^{4+}) into the less toxic chromium(III) (Cr^{3+}) ions. Subsequently, the Cr^{3+} ions (at pH 5) were easily removed without any further treatment to meet the drinking water standard.[154] Most recently, Xie et al. have demonstrated the feasibility of such an approach by removing chromate ($HCrO^{4-}$, the dominant form of chromium(IV) at neutral pH) using a hybrid NLM composed of GO and $Ti_3C_2T_x$ nanosheets.[72] In another recent study, a MXene-based catalyst (containing 20% cobalt oxide, Co_3O_4) also

demonstrated an exceptional performance for the degradation of bisphenol A, an endocrine-disruptive compound.[155] Hence, we believe that MXene-based membranes are worth investigating for the detoxification of a wide range of contaminants. Besides, as firstly demonstrated for energy applications, MXenes and their hybrids are effective (and versatile) electrocatalysts, often with extraordinary performance.[156,157] In this regard, we believe that it would be interesting to investigate the potential of MXenes for building "electroreactive" membranes, as well.

4.2. Underutilized Membrane Formats

Neither PI (phase inversion), nor IP (interfacial polymerization) has yet to be widely utilized for fabricating MXene-based membranes so far. To promote the exploration of PI and IP for MXene-based membrane research, below we share some good practices and lessons learnt from GFM-based membranes. We also provide a brief perspective on the potential utility of layer-by-layer (LbL) assembly for developing MXene-based membranes.

4.2.1. Phase Inversion

As mentioned above, we believe that polymer-MXene composites prepared either as MMMs or TFNs are more promising for realistic applications. For the preparation of both MMMs and TFNs, PI is an essential method. However, to the best of our knowledge, only Han et al. had so far reported on the utility of PI for the preparation of MXene-polymer composite membranes (PA-based MMM).[133] In their application-driven study, Han et al. briefly discussed the advantages of using PI. However, we believe there is more room for further explorations, especially on the role of the polymers, fabrication conditions, as well as the impact of MXenes on PI process itself. During PI, the MXenes (as other nanofillers) inevitably influence the phase separation behavior and hence packing of polymer chains. It had been previously shown that hydrophilic additives could facilitate the demixing process, where a solvent and coagulant (or nonsolvent) counter-diffuse in the polymer-solvent-

coagulant tertiary systems.[158,159] During the phase inversion of GFM-polymer systems, the polymer chains solidify rapidly with limited rearrangement capacity, resulting in membranes having a high surface pore density and size, as well as overall porosity.[158,160] Given their high hydrophilicity (and topological similarity to GFMs), we expect MXenes to exhibit high capacity to prepare highly permeable membranes with a wide range of polymers. Importantly, upon phase separation, MXenes will naturally be exposed to the membrane surface, which might be an interesting way to develop antibiofouling membranes. (see Section 3.2.1 for antibiofouling properties of MXenes.) On another aspect, since the phase separation process is dictated by not only the thermodynamic but also rheological factors,[161] the concentration of the MXenes should be fine-tuned in such systems. In particular, excessive use of MXenes (like other nanofillers) could also delay demixing and result in the densification of membrane structures due to the increase overall viscosity of the polymer dope solutions. Thus, it is importance to balance these two parameters to make full use of MXenes in the design of PI-based MMMs.

4.2.2. Interfacial Polymerization

IP refers to the reaction of two very reactive monomers (usually an acid chloride and an amine) at the interface of two immiscible solvents to form a dense polymeric layer (usually polyamide-based).[105] PA-based TFC membranes prepared via IP are of particular interest for a wide range of industrial separation processes. It is highly desirable to fabricate IP-based PA membranes with reduced surface roughness, increased hydrophilicity, lowered fouling propensity, and enhanced chlorine resistance. In graphene analogs, the incorporation of GO into PA membranes during IP has shown promise to achieve all these four interrelated aspects.[162] GO nanosheets are providing smoother PA layers likely by retarding the diffusion of aqueous monomers into the organic phase,[162,163] thus, we expect MXenes to exhibit a similar effect with their 2D morphology. Having

the capacity of forming strong hydrogen-bonds,[95] we also expect MXenes to be useful in preventing chloride ions from replacing amidic hydrogen and interrupt chlorination. And, as discussed above, MXenes are also antibacterial and hydrophilic like GO, which is useful for (bio)fouling control. Therefore, we think MXenes offer a good potential for designing IP-based membranes. By crosslinking MXene-incorporated PEI (hyperbranched PEI) with TMC (in n-hexane), different research groups[75,79,131] had previously created PA-based selective layers on various support membranes. From a chemical perspective, we can consider this straightforward method of IP for fabricating TFN membranes. However, the designing of IP-based TFN membranes (starting by monomers) requires more careful optimization of several parameters (e.g., choice of monomers and their concentrations, filler loading ratio, crosslinking reaction time).

4.2.3. Layer-by-Layer Assembly

Despite being less heavily emphasized than PI and IP, LbL assembly appears to be an elegant way of designing membranes. In the last couple of years, various compositions of LbL-assembled films have demonstrated promising performance as separation (as well as barrier) membranes.[164] LbL-based separation membranes typically consist of polymeric building blocks. However, the nanosheet-based or nanosheet-incorporated LbL membrane designs, which combine the advantages of LbL material design and 2DMs, are also popular (see ref.s [165,166] for GFMs-based LbL membranes.) On the other hand, MXene-incorporated LbL films have also been prepared for applications such as electromagnetic interference shielding and supercapacitive energy storage.[167,168] Thus, we expect MXene-based LbL membranes to be useful for separation/purification applications. Besides, it is worth highlighting that the LbL technique can be performed in different fashions like dipping, spinning, spraying, or a combination of those. And, the properties of the resulting films often differ drastically. Further, by playing with the deposition conditions, the properties of such films can be

fine-tuned at a molecular level. Hence, we deem LbL method promising for designing advanced separation membranes using MXenes.

4.3. Simulation/Modeling Approaches

In the wake of the fast expansion of flat materials toolbox, experimentalists have difficulties in matching the right material for the right applications, which also applies to MXenes. At this point, computer-aided materials design holds a huge promise for boosting the research outcome. Beyond, for both MXenes and their parent materials, MAX phases, computational/theoretical investigations reveal fine details of structure-property relationships that are often inaccessible or hard to study experimentally. So far, the majority of the computational studies are based on ab-initio calculations using density functional theory (DFT).[21,169–171] In the fundamental domain, those investigations covered structural, mechanical, electrical, electrochemical, and magnetic properties, as well as the nature of chemical bonding and relative stability of MXenes.[21,169,170] On the applications side, the main focus was on energy storage.[169,171] Nevertheless, as we have touched above, the electrical/electrochemical behavior of certain MXenes (e.g., $Ti_3C_2T_x$) is also very interesting for membrane applications. Thus, we would like to summarize some key points of those investigations first, followed by a couple of pioneering simulation/modeling studies directly focused on MXene-based separation membranes.

Tang et al. investigated the electronic properties of a representative MXene, Ti_3C_2 monolayers with pristine, hydroxylated, and fluorinated surfaces, and revealed clear changes in narrow-band-gap semiconducting or metallic characteristics.[169] In an early study, Kurtoglu et al. have evidenced the high metallicity and stiffness of a wide range of MXenes, comprising Ta_2C, Ta_3C_2, Ta_4C_3, Cr_2C, Zr_2C, Hf_2C, V_2C, Ti_2C, Ti_3C_2, and Ti_4C_3.[21] Within this context, Anasori et al. have later investigated MXenes containing two different transition metals (Ta, Cr, Ti, Nb, Mo, or V). These

double-transition-metal MXenes were in the form of M'M"C_2 and M'M"C_3 (**Figure 10**a), where M' and M" are the outer and inner layer metals, respectively.[170] This effort has shown the uniquely different electrochemical behavior of Mo_2TiC_2 compared to $Ti_3C_2T_x$. Critically, the researchers have supported their predictions with experimental results, as well. In a recent work, Berdiyorov et al. have employed DFT calculations for exploring the water desalination potential of MXenes.[171] They studied ionic transport through $Ti_3C_2(OH)_2$ to understand mechanisms behind charge-selectivity. They also showed that the spacing between the MXene layers expands or contracts dynamically, as a function of the charge of intercalating ions, which also alters the ionic transport behavior. As an interesting point for membrane design, the authors suggested the possibility that the performance of MXene-based ion sieving membranes could be improved by manipulating the surface terminations, which in turn, alter the surface charges.

The classical molecular simulation strategies remained relatively less explored for MXenes.[172,173] Borysiuk et al. studied the mechanical properties of $Ti_{n+1}C_n$ under tensile loading using large-scale classical molecular dynamics (MD) simulations (Figure 10b).[172] Calculated strain-stress curves showed a linear trend at small strains (≤1%), and the resulting Young's moduli were close to the data obtained previously by DFT simulations.[21] In another MD simulation study, Li et al.[173] reported on the selective diffusion of small gas molecules (He, H_2, CO_2, N_2, and CH_4) passing through two adjacent MXene sheets forming a nanogallery. They compared the gas diffusion in anhydrous and hydrated MXenes, concluding that the intercalated water molecules may increase the selectivity (towards H_2) considerably (Figure 10c). However, when water intercalation exceeded a certain concentration, the diffusion of large gas molecules dropped dramatically.

We expect simulation studies to shed more light on the transport mechanisms of MXene-based membranes in the future. In fact, the very recent contributions of Shamsabadi et al.[114] and

Wu et al.[18] on gas and liquid separations, respectively, validate this expectation. Using MD simulations, Shamsabadi et al. revealed the crucial role of interfacial interactions between PA blocks of Pebax® 1657 and $Ti_3C_2T_x$ for achieving high CO_2 permeability of resulting MMMs.[114] MD simulations also showed great utility for confirming and explaining the solvent transport in neat as well as chemically modified MXenes (i.e., $Ti_3C_2T_x$, $Ti_3C_2T_x$,-NH_2, and $Ti_3C_2T_x$-$C_{12}H_{25}$).

Going forward, MD simulations might also be instrumental for evaluating the potential of porous MXenes for membrane fabrications. MXenes are inherently layered nanosheets, even in the thinnest form (a monolayer of M_2X MXene, for example, has a quasi-trilayered structure). As a result, the point surface defects that might occur in MXene nanosheets (during etching or exfoliation) might not always result in in-plane porosity (which is not the case of truly monolayered GO, for example). Nevertheless, porous MXenes are achievable and already successfully exploited for different applications.[174,175] Accordingly, to better understand the transport behavior of MXene-based membranes and perhaps developing superior membranes that utilize porous MXenes, we also recommend MD simulations as a crucial element for further explorations.

4.4. Scale-up Potential

Putting the competitiveness assessment of their performance merits aside, MXenes, and thus naturally MXene-based membranes, are in their infancy for securely foreseeing their commercialization potential. Even most MAX phases are far from being commercially available at an affordable price at the moment, albeit there are significant efforts for producing common MAX phases in bulk quantities.[176,177] However, the scalable production of MXenes is even more challenging as there are inherent safety issues associated with fluorine-based etching chemistries.[17] The use of strong bases (e.g., sodium hydroxide, tetrabutylammonium hydroxide) as etchants,[178,179] for example, might offer a safer and hence potentially easier to scale alternative. However, the yield

and/or product quality of non-fluorine-based methods need further improvement. Also, alternative etching processes inevitably provide MXene products with significantly different surface chemical compositions. From the perspective of membrane design, this might be an opportunity to engineer the properties of membranes. On the other hand, it is important to look into scalable techniques for the processing of MXenes into membranes. For NLMs as well as MMMs, industrially acceptable methods, such as blade-casting variations,[114,180] are likely among the first choices. As discussed above in detail, PI and IP methods also worth a closer look in this regard.

5. Conclusions

Here, in this Progress Report, we put MXenes in perspective as an emerging material for the design of high-performance membranes for gas separation, water purification, and solvent purification. Among these three broad areas of separation/purification applications, gas separation is relatively less studied. Yet still, MXenes seem promising for designing gas separation membranes to operate at high temperatures. For water purification, on the other hand, MXenes offer a multitude of opportunities with their antibacterial, photothermal, and catalytic activities. MXenes have also shown a similar success so far for solvent purifications, as NLMs, as well as fillers of polymer-based composite membranes.

We have noticed that most of the studies reported so far dealt with different material systems, separation tasks, or experimental conditions. Thus, we believe there is still a large room for confirming and improving results reported for MXene-based membranes thus far. Also, except for a couple of rare examples that provide the comparisons of MXenes and GFMs, most studies focused on MXenes alone without benchmarking against alternatives under identical conditions. As a result, it is hard to compare the performance merits of MXenes with respect to other 2DMs without making too many assumptions. Accordingly, it is not clear if MXenes are superior to other 2DMs or not for

many application areas (see Table S3), which is an open question to be answered by comparative studies in the future. Despite recent efforts, it is also not clear if the oxidation issue of MXenes will limit the prospects of MXenes considerably; another open question to be addressed. On another aspect, the current literature on MXene-based membranes is clearly dominated by nanolaminates prepared via filtration-assisted film deposition methods. To fill the gap, we have proposed several future directions concerning more realistic strategies for membrane preparation, which should be of high priority as new directions for future research.

Considering the rich chemistry of MXenes, we currently exploit a very small fraction of possible MXene structures. The vast majority of existing reports on MXene-based membranes are experiment-driven, with a particular focus on titanium carbide MXene varieties. Yet still, there are attempts to involve simulation/modeling approaches to inform the designing of MXene-based membranes. We expect these efforts to intensify and help identify uncommon MXenes suitable for membrane design. Overall, we envision that MXene-based membranes will continue their fast progress made in less than half a decade in the future with growing speed. We hope that the analyses and future directions set out in this report will guide materials scientists and engineers to contribute this growth while navigating through membrane design concepts and separation applications. Likewise, we hope this Progress Report will also help membrane researchers to embrace the opportunities offered by MXenes better.

Supporting Information

Supporting Information is available from the Wiley Online Library.

Acknowledgements

T.-H. Bae would like to thank Korea Advanced Institute of Science and Technology for a financial support. Y.C. acknowledges financial support from the Australian Research Council under the Future Fellowships scheme (FT160100107) and Discovery Project (DP180102210).

Received: ((will be filled in by the editorial staff))
Revised: ((will be filled in by the editorial staff))
Published online: ((will be filled in by the editorial staff))

References

[1] M. M. Pendergast, E. M. V. Hoek, *Energy Environ. Sci.* **2011**, *4*, 1946.

[2] X. Qu, J. Brame, Q. Li, P. J. J. Alvarez, *Acc. Chem. Res.* **2013**, *46*, 834.

[3] P. S. Goh, A. F. Ismail, N. Hilal, *Desalination* **2016**, *380*, 100.

[4] Y. Manawi, V. Kochkodan, M. A. Hussein, M. A. Khaleel, M. Khraisheh, N. Hilal, *Desalination* **2016**, *391*, 69.

[5] C. Y. Chuah, K. Goh, Y. Yang, H. Gong, W. Li, H. E. Karahan, M. D. Guiver, R. Wang, T.-H. Bae, *Chem. Rev.* **2018**, *118*, 8655.

[6] G. Liu, W. Jin, N. Xu, *Chem. Soc. Rev.* **2015**, *44*, 5016.

[7] K. Goh, H. E. Karahan, L. Wei, T. Bae, A. G. Fane, R. Wang, Y. Chen, *Carbon* **2016**, *109*, 694.

[8] F. Moghadam, H. B. Park, *Curr. Opin. Chem. Eng.* **2018**, *20*, 28.

[9] J. Zhu, J. Hou, A. Uliana, Y. Zhang, M. Tian, B. Van der Bruggen, *J. Mater. Chem. A* **2018**, *6*, 3773.

[10] G. Liu, W. Jin, N. Xu, *Angew. Chemie Int. Ed.* **2016**, *55*, 13384.

[11] M. Alhabeb, K. Maleski, B. Anasori, P. Lelyukh, L. Clark, S. Sin, Y. Gogotsi, *Chem. Mater.* **2017**, *29*, 7633.

[12] Y. Gogotsi, B. Anasori, *ACS Nano* **2019**, *13*, 8491.

[13] V. H. Nowotny, *Prog. Solid State Chem.* **1971**, *5*, 27.

[14] M. W. Barsoum, *Prog. Solid State Chem.* **2000**, *28*, 201.

[15] P. Eklund, M. Beckers, U. Jansson, H. Högberg, L. Hultman, *Thin Solid Films* **2010**, *518*, 1851.

[16] M. Sokol, V. Natu, S. Kota, M. W. Barsoum, *Trends Chem.* **2019**, *1*, 210.

[17] L. Verger, V. Natu, M. Carey, M. W. Barsoum, *Trends Chem.* **2019**, *1*, 656.

[18] X. Wu, X. Cui, W. Wu, J. Wang, Y. Li, Z. Jiang, *Angew. Chemie Int. Ed.* **2019**, *58*, 18524.

[19] M. Naguib, M. Kurtoglu, V. Presser, J. Lu, J. Niu, M. Heon, L. Hultman, Y. Gogotsi, M. W. Barsoum, *Adv. Mater.* **2011**, *23*, 4248.

[20] M. Naguib, O. Mashtalir, J. Carle, V. Presser, J. Lu, L. Hultman, Y. Gogotsi, M. W. Barsoum, *ACS Nano* **2012**, *6*, 1322.

[21] M. Kurtoglu, M. Naguib, Y. Gogotsi, M. W. Barsoum, *MRS Commun.* **2012**, *2*, 133.

[22] K. Rasool, M. Helal, A. Ali, C. E. Ren, Y. Gogotsi, K. A. Mahmoud, *ACS Nano* **2016**, *10*, 3674.

[23] X.-H. Zha, J. Yin, Y. Zhou, Q. Huang, K. Luo, J. Lang, J. S. Francisco, J. He, S. Du, *J. Phys. Chem. C* **2016**, *120*, 15082.

[24] A. Lipatov, H. Lu, M. Alhabeb, B. Anasori, A. Gruverman, Y. Gogotsi, A. Sinitskii, *Sci. Adv.* **2018**, *4*, eaat0491.

[25] M. Naguib, V. N. Mochalin, M. W. Barsoum, Y. Gogotsi, *Adv. Mater.* **2014**, *26*, 992.

[26] M. Naguib, Y. Gogotsi, *Acc. Chem. Res.* **2015**, *48*, 128.

[27] V. M. Hong Ng, H. Huang, K. Zhou, P. S. Lee, W. Que, J. Z. Xu, L. B. Kong, *J. Mater. Chem. A* **2017**, *5*, 3039.

[28] M. Khazaei, A. Ranjbar, K. Esfarjani, D. Bogdanovski, R. Dronskowski, S. Yunoki, *Phys. Chem.*

Chem. Phys. **2018**, *20*, 8579.

[29] X. Xiao, H. Wang, P. Urbankowski, Y. Gogotsi, *Chem. Soc. Rev.* **2018**, *47*, 8744.

[30] M. Khazaei, A. Mishra, N. S. Venkataramanan, A. K. Singh, *Curr. Opin. Solid State Mater. Sci.* **2019**, 1.

[31] R. M. Ronchi, J. T. Arantes, S. F. Santos, *Ceram. Int.* **2019**, *45*, 18167.

[32] B. Anasori, M. R. Lukatskaya, Y. Gogotsi, *Nat. Rev. Mater.* **2017**, *2*, 16098.

[33] H. Wang, Y. Wu, X. Yuan, G. Zeng, J. Zhou, X. Wang, J. W. Chew, *Adv. Mater.* **2018**, *30*, 1704561.

[34] X. Li, C. Wang, Y. Cao, G. Wang, *Chem. - An Asian J.* **2018**, *13*, 2742.

[35] J. Pang, R. G. Mendes, A. Bachmatiuk, L. Zhao, H. Q. Ta, T. Gemming, H. Liu, Z. Liu, M. H. Rummeli, *Chem. Soc. Rev.* **2019**, *48*, 72.

[36] C. (John) Zhang, Y. Ma, X. Zhang, S. Abdolhosseinzadeh, H. Sheng, W. Lan, A. Pakdel, J. Heier, F. Nüesch, *Energy Environ. Mater.* **2019**, eem2.12058.

[37] J. Zhu, E. Ha, G. Zhao, Y. Zhou, D. Huang, G. Yue, L. Hu, N. Sun, Y. Wang, L. Y. S. Lee, C. Xu, K.-Y. Wong, D. Astruc, P. Zhao, *Coord. Chem. Rev.* **2017**, *352*, 306.

[38] H. Lin, Y. Chen, J. Shi, *Adv. Sci.* **2018**, *5*, 1800518.

[39] K. Huang, Z. Li, J. Lin, G. Han, P. Huang, *Chem. Soc. Rev.* **2018**, *47*, 5109.

[40] M. Soleymaniha, M.-A. Shahbazi, A. R. Rafieerad, A. Maleki, A. Amiri, *Adv. Healthc. Mater.* **2018**, 1801137.

[41] Y. Zhang, L. Wang, N. Zhang, Z. Zhou, *RSC Adv.* **2018**, *8*, 19895.

[42] B.-M. Jun, S. Kim, J. Heo, C. M. Park, N. Her, M. Jang, Y. Huang, J. Han, Y. Yoon, *Nano Res.* **2019**, *12*, 471.

[43] L. Huang, H. Lin, *Membranes* **2018**, *8*, 100.

[44] S. Kim, H. Wang, Y. M. Lee, *Angew. Chemie Int. Ed.* **2019**, DOI 10.1002/anie.201814349.

[45] Y. Kang, Y. Xia, H. Wang, X. Zhang, *Adv. Funct. Mater.* **2019**, *29*, 1902014.

[46] T. Hyun, J. Jeong, A. Chae, Y. K. Kim, D.-Y. Koh, *BMC Chem. Eng.* **2019**, *1*, 12.

[47] K. Rasool, R. P. Pandey, P. A. Rasheed, S. Buczek, Y. Gogotsi, K. A. Mahmoud, *Mater. Today* **2019**, DOI 10.1016/j.mattod.2019.05.017.

[48] P. Srimuk, F. Kaasik, B. Krüner, A. Tolosa, S. Fleischmann, N. Jäckel, M. C. Tekeli, M. Aslan, M. E. Suss, V. Presser, *J. Mater. Chem. A* **2016**, *4*, 18265.

[49] W. Bao, X. Tang, X. Guo, S. Choi, C. Wang, Y. Gogotsi, G. Wang, *Joule* **2018**, *2*, 778.

[50] Q. Zhang, J. Teng, G. Zou, Q. Peng, Q. Du, T. Jiao, J. Xiang, *Nanoscale* **2016**, *8*, 7085.

[51] A. Shahzad, K. Rasool, W. Miran, M. Nawaz, J. Jang, K. A. Mahmoud, D. S. Lee, *ACS Sustain. Chem. Eng.* **2017**, *5*, 11481.

[52] N.-N. Wang, H. Wang, Y. Wang, Y. Wei, J. Si, A. C. Y. Yuen, J. Xie, B. Yu, S. Zhu, H. Lu, W. Yang, Q. N. Chan, G. Yeoh, *ACS Appl. Mater. Interfaces* **2019**, *11*, 40512.

[53] C. Xu, L. Wang, Z. Liu, L. Chen, J. Guo, N. Kang, X.-L. Ma, H.-M. Cheng, W. Ren, *Nat. Mater.* **2015**, *14*, 1135.

[54] J. Zhou, X. Zha, F. Y. Chen, Q. Ye, P. Eklund, S. Du, Q. Huang, *Angew. Chemie Int. Ed.* **2016**, *55*, 5008.

[55] J. Zhou, X. Zha, X. Zhou, F. Chen, G. Gao, S. Wang, C. Shen, T. Chen, C. Zhi, P. Eklund, S. Du, J. Xue, W. Shi, Z. Chai, Q. Huang, *ACS Nano* **2017**, *11*, 3841.

[56] M. Malaki, A. Maleki, R. S. Varma, *J. Mater. Chem. A* **2019**, *7*, 10843.

[57] M. Naguib, J. Come, B. Dyatkin, V. Presser, P. L. Taberna, P. Simon, M. W. Barsoum, Y. Gogotsi, *Electrochem. Commun.* **2012**, *16*, 61.

[58] C. Li, S. Kota, C. Hu, M. W. Barsoum, *J. Ceram. Sci. Technol.* **2016**, *7*, 301.

[59] M. Alhabeb, K. Maleski, T. S. Mathis, A. Sarycheva, C. B. Hatter, S. Uzun, A. Levitt, Y. Gogotsi, *Angew. Chemie Int. Ed.* **2018**, *57*, 5444.

[60] C. E. Ren, K. B. Hatzell, M. Alhabeb, Z. Ling, K. A. Mahmoud, Y. Gogotsi, *J. Phys. Chem. Lett.* **2015**, *6*, 4026.

[61] J. Halim, M. R. Lukatskaya, K. M. Cook, J. Lu, C. R. Smith, L.-Å. Näslund, S. J. May, L. Hultman, Y. Gogotsi, P. Eklund, M. W. Barsoum, *Chem. Mater.* **2014**, *26*, 2374.

[62] L. H. Karlsson, J. Birch, J. Halim, M. W. Barsoum, P. O. Å. Persson, *Nano Lett.* **2015**, *15*, 4955.

[63] L. Wang, H. Zhang, B. Wang, C. Shen, C. Zhang, Q. Hu, A. Zhou, B. Liu, *Electron. Mater. Lett.* **2016**, *12*, 702.

[64] C. J. Zhang, M. P. Kremer, A. Seral-Ascaso, S.-H. Park, N. McEvoy, B. Anasori, Y. Gogotsi, V. Nicolosi, *Adv. Funct. Mater.* **2018**, *28*, 1705506.

[65] P. Lakhe, E. M. Prehn, T. Habib, J. L. Lutkenhaus, M. Radovic, M. S. Mannan, M. J. Green, *Ind.*

Eng. Chem. Res. **2019**, *58*, 1570.

[66] F. Du, H. Tang, L. Pan, T. Zhang, H. Lu, J. Xiong, J. Yang, C. (John) Zhang, *Electrochim. Acta* **2017**, *235*, 690.

[67] C. Zhang, S.-H. Park, A. Seral‐Ascaso, S. Barwich, N. McEvoy, C. S. Boland, J. N. Coleman, Y. Gogotsi, V. Nicolosi, *Nat. Commun.* **2019**, *10*, 849.

[68] C. J. Zhang, B. Anasori, A. Seral-Ascaso, S.-H. Park, N. McEvoy, A. Shmeliov, G. S. Duesberg, J. N. Coleman, Y. Gogotsi, V. Nicolosi, *Adv. Mater.* **2017**, *29*, 1702678.

[69] C. J. Zhang, S. Pinilla, N. McEvoy, C. P. Cullen, B. Anasori, E. Long, S.-H. Park, A. Seral-Ascaso, A. Shmeliov, D. Krishnan, C. Morant, X. Liu, G. S. Duesberg, Y. Gogotsi, V. Nicolosi, *Chem. Mater.* **2017**, *29*, 4848.

[70] J. Shen, G. Liu, Y. Ji, Q. Liu, L. Cheng, K. Guan, M. Zhang, G. Liu, J. Xiong, J. Yang, W. Jin, *Adv. Funct. Mater.* **2018**, *28*, 1801511.

[71] L. Ding, Y. Wei, Y. Wang, H. Chen, J. Caro, H. Wang, *Angew. Chemie Int. Ed.* **2017**, *56*, 1825.

[72] X. Xie, C. Chen, N. Zhang, Z.-R. Tang, J. Jiang, Y.-J. Xu, *Nat. Sustain.* **2019**, *2*, 856.

[73] G. Liu, L. Cheng, G. Chen, F. Liang, G. Liu, W. Jin, *Chem. – An Asian J.* **2019**, inpress.

[74] M. A. Hope, A. C. Forse, K. J. Griffith, M. R. Lukatskaya, M. Ghidiu, Y. Gogotsi, C. P. Grey, *Phys. Chem. Chem. Phys.* **2016**, *18*, 5099.

[75] X. Wu, L. Hao, J. Zhang, X. Zhang, J. Wang, J. Liu, *J. Membr. Sci.* **2016**, *515*, 175.

[76] J. Luo, W. Zhang, H. Yuan, C. Jin, L. Zhang, H. Huang, C. Liang, Y. Xia, J. Zhang, Y. Gan, X. Tao, *ACS Nano* **2017**, *11*, 2459.

[77] Z. Huang, S. Wang, S. Kota, Q. Pan, M. W. Barsoum, C. Y. Li, *Polymer* **2016**, *102*, 119.

[78] Z. Ling, C. E. Ren, M.-Q. Zhao, J. Yang, J. M. Giammarco, J. Qiu, M. W. Barsoum, Y. Gogotsi, *Proc. Natl. Acad. Sci.* **2014**, *111*, 16676.

[79] L. Hao, H. Zhang, X. Wu, J. Zhang, J. Wang, Y. Li, *Compos. Part A Appl. Sci. Manuf.* **2017**, *100*, 139.

[80] K. Wang, Y. Zhou, W. Xu, D. Huang, Z. Wang, M. Hong, *Ceram. Int.* **2016**, *42*, 8419.

[81] D. Xiong, X. Li, Z. Bai, S. Lu, *Small* **2018**, *14*, 1703419.

[82] T. Habib, X. Zhao, S. A. Shah, Y. Chen, W. Sun, H. An, J. L. Lutkenhaus, M. Radovic, M. J. Green, *npj 2D Mater. Appl.* **2019**, *3*, 8.

[83] Y. Lee, S. J. Kim, Y.-J. Kim, Y. Lim, Y. Chae, B.-J. Lee, Y.-T. Kim, H. Han, Y. Gogotsi, A. Chi Won, *J. Mater. Chem. A* **2019**, DOI 10.1039/C9TA07036B.

[84] C. E. Ren, M. Alhabeb, B. W. Byles, M.-Q. Zhao, B. Anasori, E. Pomerantseva, K. A. Mahmoud, Y. Gogotsi, *ACS Appl. Nano Mater.* **2018**, *1*, 3644.

[85] K. Rasool, K. A. Mahmoud, D. J. Johnson, M. Helal, G. R. Berdiyorov, Y. Gogotsi, *Sci. Rep.* **2017**, *7*, 1598.

[86] R. P. Pandey, K. Rasool, V. E. Madhavan, B. Aïssa, Y. Gogotsi, K. A. Mahmoud, *J. Mater. Chem. A* **2018**, *6*, 3522.

[87] X. Gao, Z.-K. Li, J. Xue, Y. Qian, L.-Z. Zhang, J. Caro, H. Wang, *J. Membr. Sci.* **2019**, *586*, 162.

[88] V. Natu, M. Sokol, L. Verger, M. W. Barsoum, *J. Phys. Chem. C* **2018**, *122*, 27745.

[89] L. Ding, Y. Wei, L. Li, T. Zhang, H. Wang, J. Xue, L.-X. Ding, S. Wang, J. Caro, Y. Gogotsi, *Nat.*

Commun. **2018**, *9*, 155.

[90] W. L. Xu, C. Fang, F. Zhou, Z. Song, Q. Liu, R. Qiao, M. Yu, *Nano Lett.* **2017**, *17*, 2928.

[91] H. Zhou, Y. Wang, F. Wang, H. Deng, Y. Song, C. Li, Z. Ling, *Chinese Chem. Lett.* **2019**, inpress.

[92] Z. Xu, Y. Sun, Y. Zhuang, W. Jing, H. Ye, Z. Cui, *J. Membr. Sci.* **2018**, *564*, 35.

[93] B. Akuzum, K. Maleski, B. Anasori, P. Lelyukh, N. J. Alvarez, E. C. Kumbur, Y. Gogotsi, *ACS Nano* **2018**, *12*, 2685.

[94] K. M. Kang, D. W. Kim, C. E. Ren, K. M. Cho, S. J. Kim, J. H. Choi, Y. T. Nam, Y. Gogotsi, H.-T. Jung, *ACS Appl. Mater. Interfaces* **2017**, *9*, 44687.

[95] K. Maleski, V. N. Mochalin, Y. Gogotsi, *Chem. Mater.* **2017**, *29*, 1632.

[96] Z. Xu, G. Liu, H. Ye, W. Jin, Z. Cui, *J. Membr. Sci.* **2018**, *563*, 625.

[97] Q. Luan, Y. Xie, D. Teng, R. Han, S. Zhang, *Desalin. Water Treat.* **2018**, *108*, 90.

[98] R. Mahajan, W. J. Koros, M. Thundyil, *Membr. Technol.* **1999**, *1999*, 6.

[99] T.-S. Chung, L. Y. Jiang, Y. Li, S. Kulprathipanja, *Prog. Polym. Sci.* **2007**, *32*, 483.

[100] M. A. Aroon, A. F. Ismail, T. Matsuura, M. M. Montazer-Rahmati, *Sep. Purif. Technol.* **2010**, *75*, 229.

[101] D. Qadir, H. Mukhtar, L. K. Keong, *Sep. Purif. Rev.* **2017**, *46*, 62.

[102] Jin, Fan, Meng, Zhang, Meng, Yang, Liu, *Processes* **2019**, *7*, 751.

[103] L. M. Robeson, *J. Membr. Sci.* **2008**, *320*, 390.

[104] J. G. Wijmans, R. W. Baker, *J. Membr. Sci.* **1995**, *107*, 1.

[105] M. Mulder, *Basic Principles of Membrane Technology*, Springer Netherlands, Dordrecht, **1996**.

[106] M. Galizia, W. S. Chi, Z. P. Smith, T. C. Merkel, R. W. Baker, B. D. Freeman, *Macromolecules* **2017**, *50*, 7809.

[107] A. G. Fane, R. Wang, M. X. Hu, *Angew. Chemie Int. Ed.* **2015**, *54*, 3368.

[108] J. M. . Peeters, J. . Boom, M. H. . Mulder, H. Strathmann, *J. Membr. Sci.* **1998**, *145*, 199.

[109] J. Wang, P. Chen, B. Shi, W. Guo, M. Jaroniec, S.-Z. Z. Qiao, *Angew. Chemie Int. Ed.* **2018**, *57*, 6814.

[110] J. A. Mason, T. M. McDonald, T.-H. Bae, J. E. Bachman, K. Sumida, J. J. Dutton, S. S. Kaye, J. R. Long, *J. Am. Chem. Soc.* **2015**, *137*, 4787.

[111] Y. Yang, C. Y. Chuah, H. Gong, T.-H. Bae, *J. CO2 Util.* **2017**, *19*, 214.

[112] Y. Yang, C. Y. Chuah, T.-H. Bae, *Chem. Eng. J.* **2019**, *358*, 1227.

[113] Y. Fan, L. Wei, X. Meng, W. Zhang, N. Yang, Y. Jin, X. Wang, M. Zhao, S. Liu, *J. Membr. Sci.* **2019**, *569*, 117.

[114] A. A. Shamsabadi, A. Pournaghshband Isfahani, S. Khoshhal Salestan, A. Rahimpour, B. Ghalei, E. Sivaniah, M. Soroush, *ACS Appl. Mater. Interfaces* **2019**, inpress.

[115] National Research Council, in *Comp. Dosim. Radon Mines Homes*, National Academies Press, Washington, D.C., **1991**.

[116] T. Liu, X. Liu, N. Graham, W. Yu, K. Sun, *J. Membr. Sci.* **2020**, *593*, 117431.

[117] Y. Sun, Z. Xu, Y. Zhuang, G. Liu, W. Jin, G. Liu, W. Jing, *2D Mater.* **2018**, *5*, 045003.

[118] F. Alimohammadi, M. Sharifian, N. H. Attanayake, A. C. Thenuwara, Y. Gogotsi, B. Anasori, D. R. Strongin, *Langmuir* **2018**, *34*, 7192.

[119] J. Saththasivam, K. Wang, W. Yiming, Z. Liu, K. A. Mahmoud, *RSC Adv.* **2019**, *9*, 16296.

[120] Z.-K. Li, Y. Liu, L. Li, Y. Wei, J. Caro, H. Wang, *J. Membr. Sci.* **2019**, *592*, 117361.

[121] R. Han, X. Ma, Y. Xie, D. Teng, S. Zhang, *RSC Adv.* **2017**, *7*, 56204.

[122] B. Mi, *Science* **2014**, *343*, 740.

[123] Y. Sun, S. Li, Y. Zhuang, G. Liu, W. Xing, W. Jing, *J. Membr. Sci.* **2019**, *591*, 117350.

[124] Z. Lu, Y. Wei, J. Deng, L. Ding, Z. Li, H. Wang, *ACS Nano* **2019**, *13*, 10535.

[125] R. Li, L. Zhang, L. Shi, P. Wang, *ACS Nano* **2017**, *11*, 3752.

[126] J. Zhao, Y. Yang, C. Yang, Y. Tian, Y. Han, J. Liu, X. Yin, W. Que, *J. Mater. Chem. A* **2018**, *6*, 16196.

[127] Y. Z. Tan, H. Wang, L. Han, M. B. Tanis-Kanbur, M. V. Pranav, J. W. Chew, *J. Membr. Sci.* **2018**, *565*, 254.

[128] X. Zha, X. Zhao, J. Pu, L. Tang, K. Ke, R. Bao, L. Bai, Z. Liu, M.-B. Yang, W. Yang, *ACS Appl. Mater. Interfaces* **2019**, *11*, 36589.

[129] A. Zandiatashbar, G. H. Lee, S. J. An, S. Lee, N. Mathew, M. Terrones, T. Hayashi, C. R. Picu, J. Hone, N. Koratkar, *Nat. Commun.* **2014**, *5*, 1.

[130] S. Wei, Y. Xie, Y. Xing, L. Wang, H. Ye, X. Xiong, S. Wang, K. Han, *J. Membr. Sci.* **2019**, *582*, 414.

[131] G. Liu, J. Shen, Y. Ji, Q. Liu, G. Liu, J. Yang, W. Jin, *J. Mater. Chem. A* **2019**, *7*, 12095.

[132] Y. Wu, L. Ding, Z. Lu, J. Deng, Y. Wei, *J. Membr. Sci.* **2019**, *590*, 117300.

[133] R. Han, Y. Xie, X. Ma, *Chinese J. Chem. Eng.* **2019**, *27*, 877.

[134] A. Ronen, S. L. Walker, D. Jassby, *Rev. Chem. Eng.* **2016**, *32*, 533.

[135] P. Formoso, E. Pantuso, G. De Filpo, F. Nicoletta, *Membranes* **2017**, *7*, 39.

[136] S.-C. Low, O.-H. Ng, in *Adv. Nanomater. Membr. Synth. Its Appl.*, Elsevier, **2019**, pp. 69–99.

[137] Y. Luo, G. Chen, X. Chen, H. Wang, Y. Luo, G. Chen, L. Ding, X. Chen, L. Ding, H. Wang, *Joule* **2019**, *3*, 279.

[138] A. Sinopoli, Z. Othman, K. Rasool, K. A. Mahmoud, *Curr. Opin. Solid State Mater. Sci.* **2019**, inpress.

[139] L. Agartan, K. Hantanasirisakul, S. Buczek, B. Akuzum, K. A. Mahmoud, B. Anasori, Y. Gogotsi, E. C. Kumbur, *Desalination* **2020**, *477*, 114267.

[140] J. Lao, R. Lv, J. Gao, A. Wang, J. Wu, J. Luo, *ACS Nano* **2018**, *12*, 12464.

[141] Z. Zhang, S. Yang, P. Zhang, J. Zhang, G. Chen, X. Feng, *Nat. Commun.* **2019**, *10*, 2920.

[142] J. Zhang, Y. Liu, Z. Lv, T. Zhao, P. Li, Y. Sun, J. Wang, *Solid State Ionics* **2017**, *310*, 100.

[143] M. Fei, R. Lin, Y. Deng, H. Xian, R. Bian, X. Zhang, J. Cheng, C. Xu, D. Cai, *Nanotechnology* **2018**, *29*, 035403.

[144] X. Zhang, C. Fan, N. Yao, P. Zhang, T. Hong, C. Xu, J. Cheng, *J. Membr. Sci.* **2018**, *563*, 882.

[145] C. Cheng, X. Zhang, Z. Yang, *J. Phys. Condens. Matter* **2019**, *31*, 215201.

[146] C. Lin, W. Zhang, L. Wang, Z. Wang, W. Zhao, W. Duan, Z. Zhao, B. Liu, J. Jin, *J. Mater. Chem. A*

2016, *4*, 5993.

[147] L. Yin, G. Xu, P. Nie, H. Dou, X. Zhang, *Chem. Eng. J.* **2018**, *352*, 695.

[148] J. Wang, P. Zhai, T. Zhao, M. Li, Z. Yang, H. Zhang, J. Huang, *Electrochim. Acta* **2019**, *320*, 134558.

[149] H. Zhan, Z. Xiong, C. Cheng, Q. Liang, J. Z. Liu, D. Li, *Adv. Mater.* **2019**, 1904562.

[150] J. Kim, B. Van der Bruggen, *Environ. Pollut.* **2010**, *158*, 2335.

[151] S. R. Lewis, S. Datta, M. Gui, E. L. Coker, F. E. Huggins, S. Daunert, L. Bachas, D. Bhattacharyya, *Proc. Natl. Acad. Sci. U. S. A.* **2011**, *108*, 8577.

[152] M. Gui, L. E. Ormsbee, D. Bhattacharyya, *Ind. Eng. Chem. Res.* **2013**, *52*, 10430.

[153] R. P. Pandey, K. Rasool, P. Abdul Rasheed, K. A. Mahmoud, *ACS Sustain. Chem. Eng.* **2018**, *6*, 7910.

[154] Y. Ying, Y. Liu, X. Wang, Y. Mao, W. Cao, P. Hu, X. Peng, *ACS Appl. Mater. Interfaces* **2015**, *7*, 1795.

[155] Y. Liu, R. Luo, Y. Li, J. Qi, C. Wang, J. Li, X. Sun, L. Wang, *Chem. Eng. J.* **2018**, *347*, 731.

[156] Z. Zhang, H. Li, G. Zou, C. Fernandez, B. Liu, Q. Zhang, J. Hu, Q. Peng, *ACS Sustain. Chem. Eng.* **2016**, *4*, 6763.

[157] Q. Xue, Z. Pei, Y. Huang, M. Zhu, Z. Tang, H. Li, Y. Huang, N. Li, H. Zhang, C. Zhi, *J. Mater. Chem. A* **2017**, *5*, 20818.

[158] J. Lee, H. Chae, Y. J. Won, K. Lee, C.-H. Lee, H. H. Lee, I. Kim, J. Lee, *J. Membr. Sci.* **2013**, *448*, 223.

[159] J.-H. Choi, J. Jegal, W.-N. Kim, *J. Membr. Sci.* **2006**, *284*, 406.

[160] S. Leaper, A. Abdel-Karim, B. Faki, J. M. Luque-Alled, M. Alberto, A. Vijayaraghavan, S. M. Holmes, G. Szekely, M. I. Badawy, N. Shokri, P. Gorgojo, *J. Membr. Sci.* **2018**, *554*, 309.

[161] J. Lee, R. Wang, T.-H. Bae, *Desalination* **2018**, *436*, 48.

[162] H.-R. Chae, J. Lee, C.-H. Lee, I.-C. Kim, P.-K. Park, *J. Membr. Sci.* **2015**, *483*, 128.

[163] A. K. Ghosh, E. M. V. Hoek, *J. Membr. Sci.* **2009**, *336*, 140.

[164] N. Joseph, P. Ahmadiannamini, R. Hoogenboom, I. F. J. Vankelecom, *Polym. Chem.* **2014**, *5*, 1817.

[165] W. Choi, J. Choi, J. Bang, J.-H. Lee, *ACS Appl. Mater. Interfaces* **2013**, *5*, 12510.

[166] M. Hu, B. Mi, *Environ. Sci. Technol.* **2013**, *47*, 3715.

[167] G.-M. Weng, J. Li, M. Alhabeb, C. Karpovich, H. Wang, J. Lipton, K. Maleski, J. Kong, E. Shaulsky, M. Elimelech, Y. Gogotsi, A. D. Taylor, *Adv. Funct. Mater.* **2018**, *28*, 1803360.

[168] Z. Zhou, W. Panatdasirisuk, T. S. Mathis, B. Anasori, C. Lu, X. Zhang, Z. Liao, Y. Gogotsi, S. Yang, *Nanoscale* **2018**, *10*, 6005.

[169] Q. Tang, Z. Zhou, P. Shen, *J. Am. Chem. Soc.* **2012**, *134*, 16909.

[170] B. Anasori, Y. Xie, M. Beidaghi, J. Lu, B. C. Hosler, L. Hultman, P. R. C. Kent, Y. Gogotsi, M. W. Barsoum, *ACS Nano* **2015**, *9*, 9507.

[171] G. R. Berdiyorov, M. E. Madjet, K. A. Mahmoud, *Appl. Phys. Lett.* **2016**, *108*, 113110.

[172] V. N. Borysiuk, V. N. Mochalin, Y. Gogotsi, *Nanotechnology* **2015**, *26*, 265705.

[173] L. Li, T. Zhang, Y. Duan, Y. Wei, C. Dong, L. Ding, Z. Qiao, H. Wang, *J. Mater. Chem. A* **2018**, *6*, 11734.

[174] C. E. Ren, M.-Q. Zhao, T. Makaryan, J. Halim, M. Boota, S. Kota, B. Anasori, M. W. Barsoum, Y. Gogotsi, *ChemElectroChem* **2016**, *3*, 689.

[175] M. Mojtabavi, A. VahidMohammadi, W. Liang, M. Beidaghi, M. Wanunu, *ACS Nano* **2019**, *13*, 3042.

[176] M. Radovic, M. W. Barsoum, *Am. Ceram. Soc. Bull.* **2013**, *92*, 20.

[177] M. W. Barsoum, P. Eklund, in *2D Met. Carbides Nitrides*, Springer International Publishing, Cham, **2019**, pp. 15–35.

[178] M. Naguib, R. R. Unocic, B. L. Armstrong, J. Nanda, *Dalt. Trans.* **2015**, *44*, 9353.

[179] T. Li, L. Yao, Q. Liu, J. Gu, R. Luo, J. Li, X. Yan, W. Wang, P. Liu, B. Chen, W. Zhang, W. Abbas, R. Naz, D. Zhang, *Angew. Chemie Int. Ed.* **2018**, *57*, 6115.

[180] E. Yang, H. E. Karahan, K. Goh, C. Y. Chuah, R. Wang, T.-H. Bae, *Carbon* **2019**, *155*, 129.

[181] G. Liu, J. Shen, Q. Liu, G. Liu, J. Xiong, J. Yang, W. Jin, *J. Membr. Sci.* **2018**, *548*, 548.

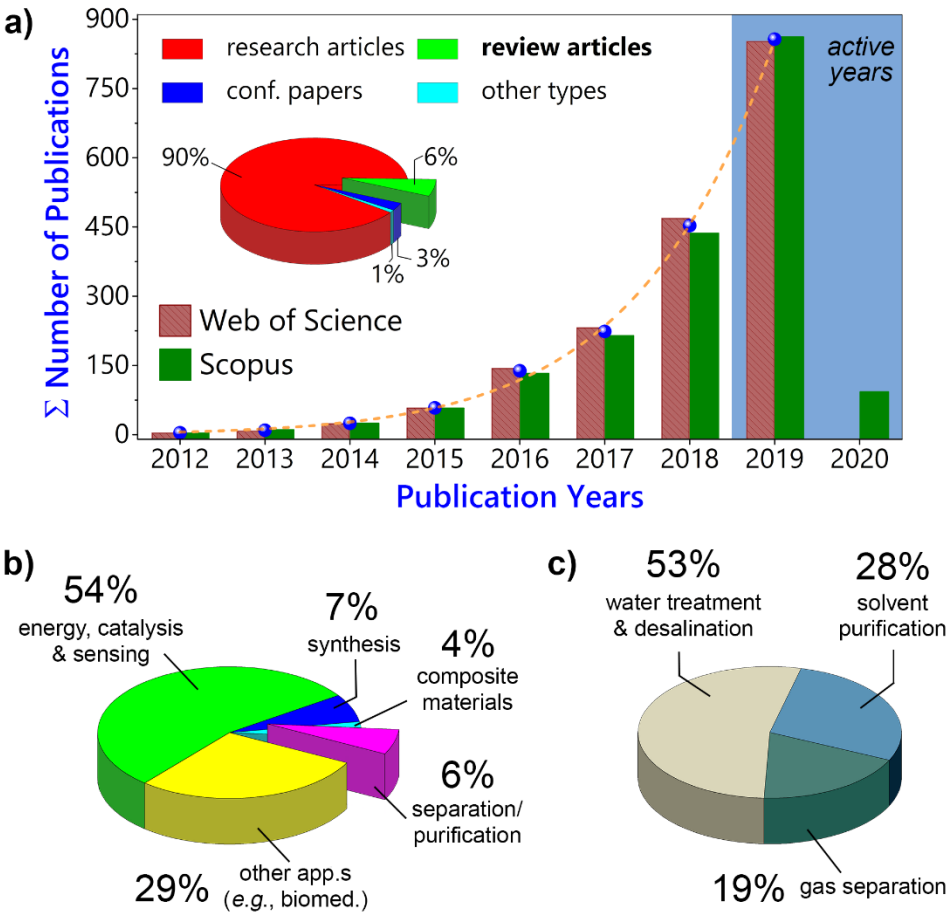

Figure 1. The expansion and topical distribution of MXene literature as of 01.Jan.2020: (a) Growth of MXenes based on Scopus® and Web of Science databases (excluding patents); (b,c) Topic-based distribution of MXene literature according to the number of published articles (b) in all fields, and (c) in experimental research on membrane-based separations only. (Note that we have considered the primary focuses of the publications in Figure 1b and Figure 1c. The "separation/purification" share of the pie as seen in Figure 1b also includes applications such as capacitive deionization,[48,49] adsorptive or reactive detoxification of water contaminants,[50,51] and oil/water separation by aerogels.[52])

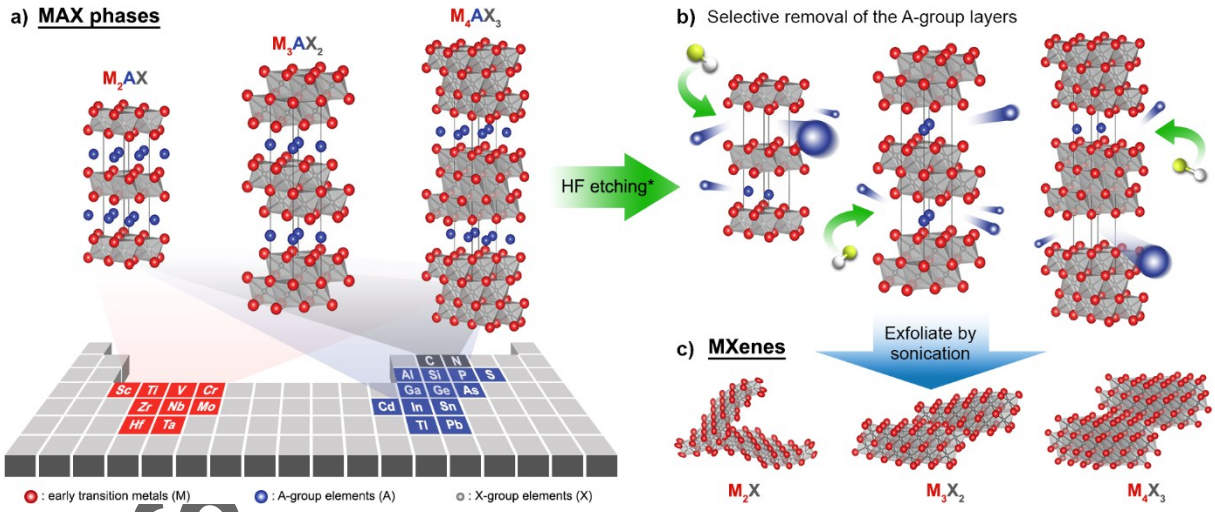

Figure 2. A typical synthetic route for producing common variations of MXene nanosheets, starting from (a) MAX phases, with different structures comprising different elements, undergoing (b) HF etching to selectively remove the A-group layers from the MAX phases before (c) a final sonication step to exfoliate out the different types of MXene nanosheets. * For the synthesis of MXenes starting by HF etching of non-MAX precursors, the interested reader may refer to ref.s [54,55]. Adapted with permission.[25] Copyright 2013, Wiley-VCH.

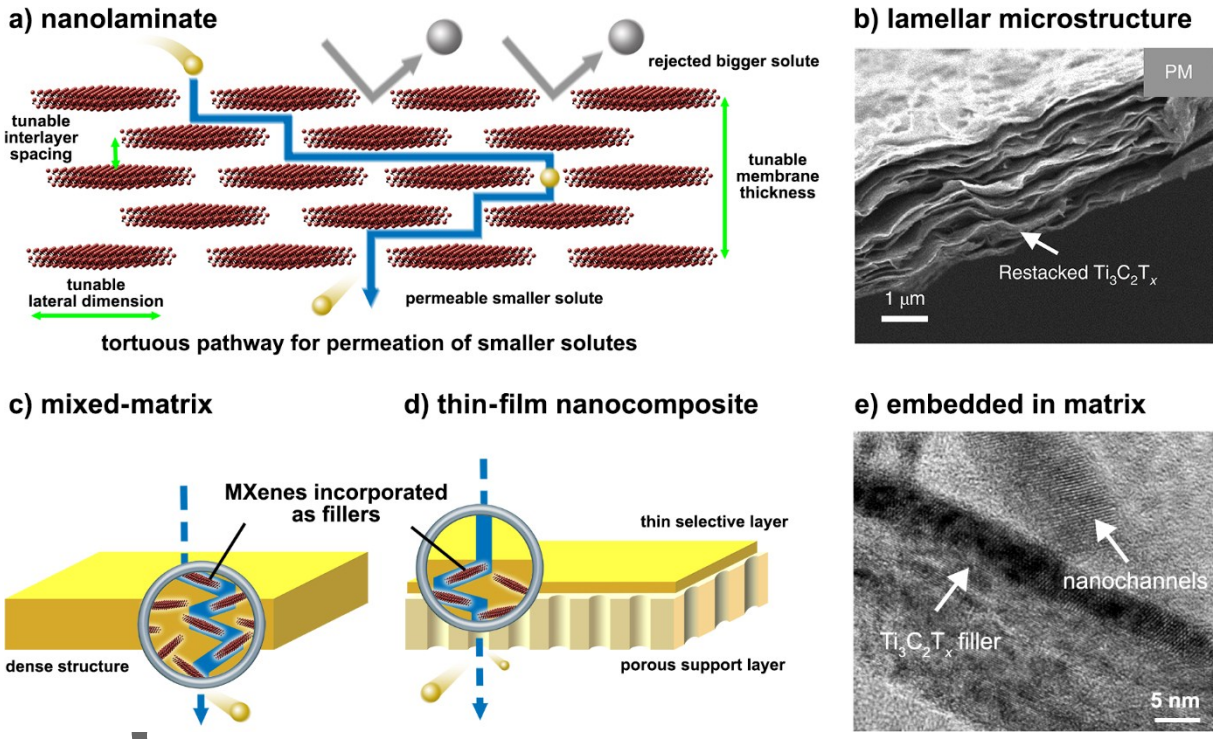

Figure 3. Schematic illustrations and representative micrographs of major membrane formats used for fabricating MXene-based membranes. (a) Illustration of solute transport through a MXene-based NLM. (b) A representative electron micrograph of MXene-based NLM. (a,b) Reproduced with permission.[72] Copyright 2019, Springer Nature. (c) MMMs and (d) TFNs formed by using MXene nanosheets as filler materials incorporated (c) in bulk polymer matrices or (d) thin selective layers over a porous support. (e) A representative micrograph of a MXene nanosheet embedded in polymer matrix. (c-e) Reproduced with permission.[73] Copyright 2019, Wiley-VCH. (Note that the tortuous pathways idealized in Figure 3a can be tailored by tuning several parameters such as the interlayer spacing, lateral dimension, and overall thickness of membranes.)

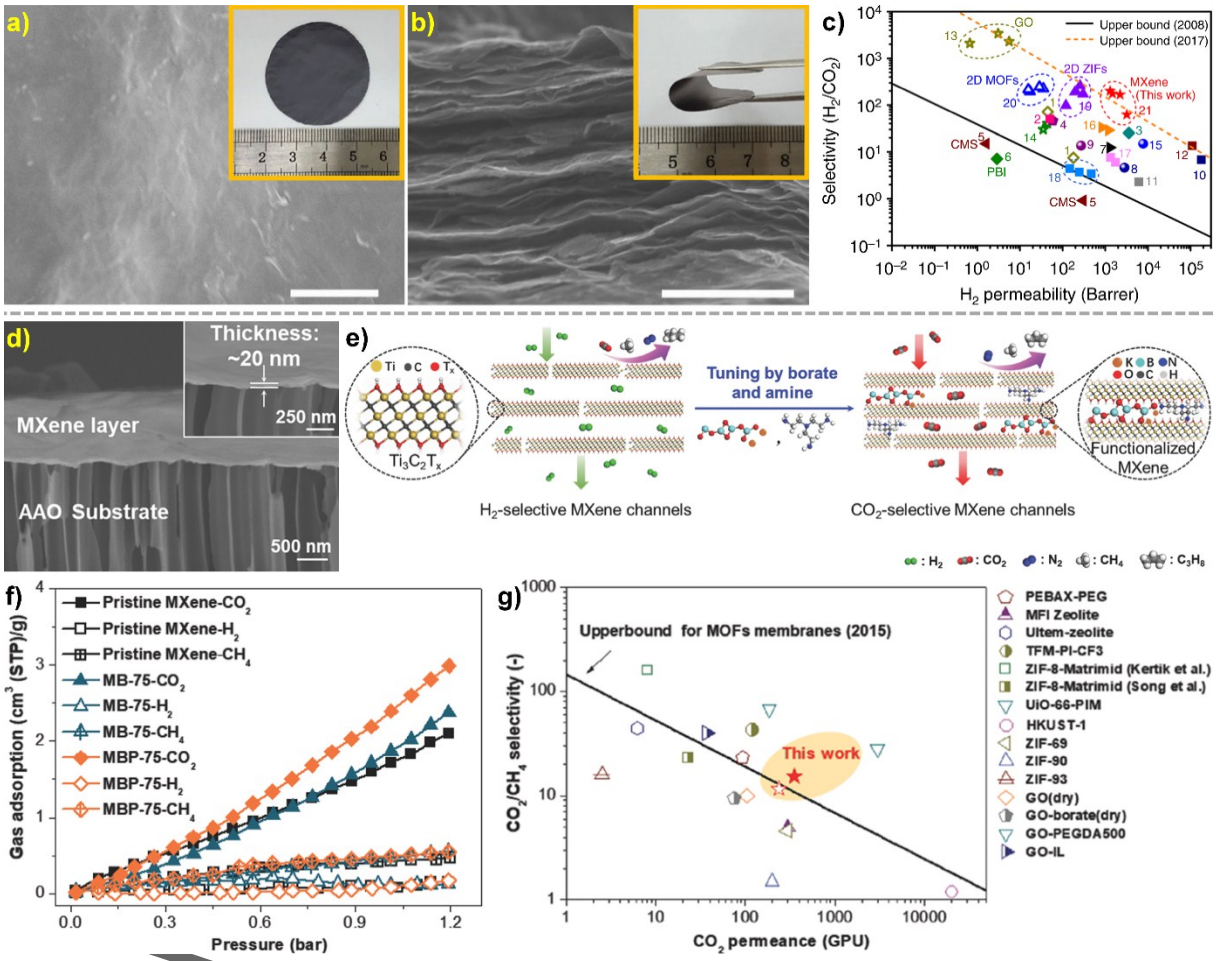

Figure 4. Gas separation performance of MXene-based membranes. (a) Top and (b) cross-sectional SEM images of a free-standing MXene membrane (inset: photograph of the same membrane); (inset: photograph of the same membrane when in the tweezer-bent state); (c) H_2/CO_2 separation performance of the MXene membrane in Robeson-type plot. (a-c) Reproduced under the terms of a Creative Commons Attribution 4.0 International License.[89] Copyright 2018, The Authors, published by Springer Nature. (d) A MXene NLM deposited on AAO support; (e) Depiction of the structure and gas transport behavior of H_2- and CO_2-selective MXene nanolaminate; (f) Gas adsorption properties of MXene-based nanolaminates (MB: MXenes crosslinked with borate; MBP: MXenes crosslinked/intercalated with borate and PEI) at 25 °C; (g) CO_2/CH_4 separation performance of MBP-75 nanolaminate ("75" denotes the treatment temperature in °C). (d-h) Reproduced with permission.[70] Copyright 2017, Wiley-VCH.

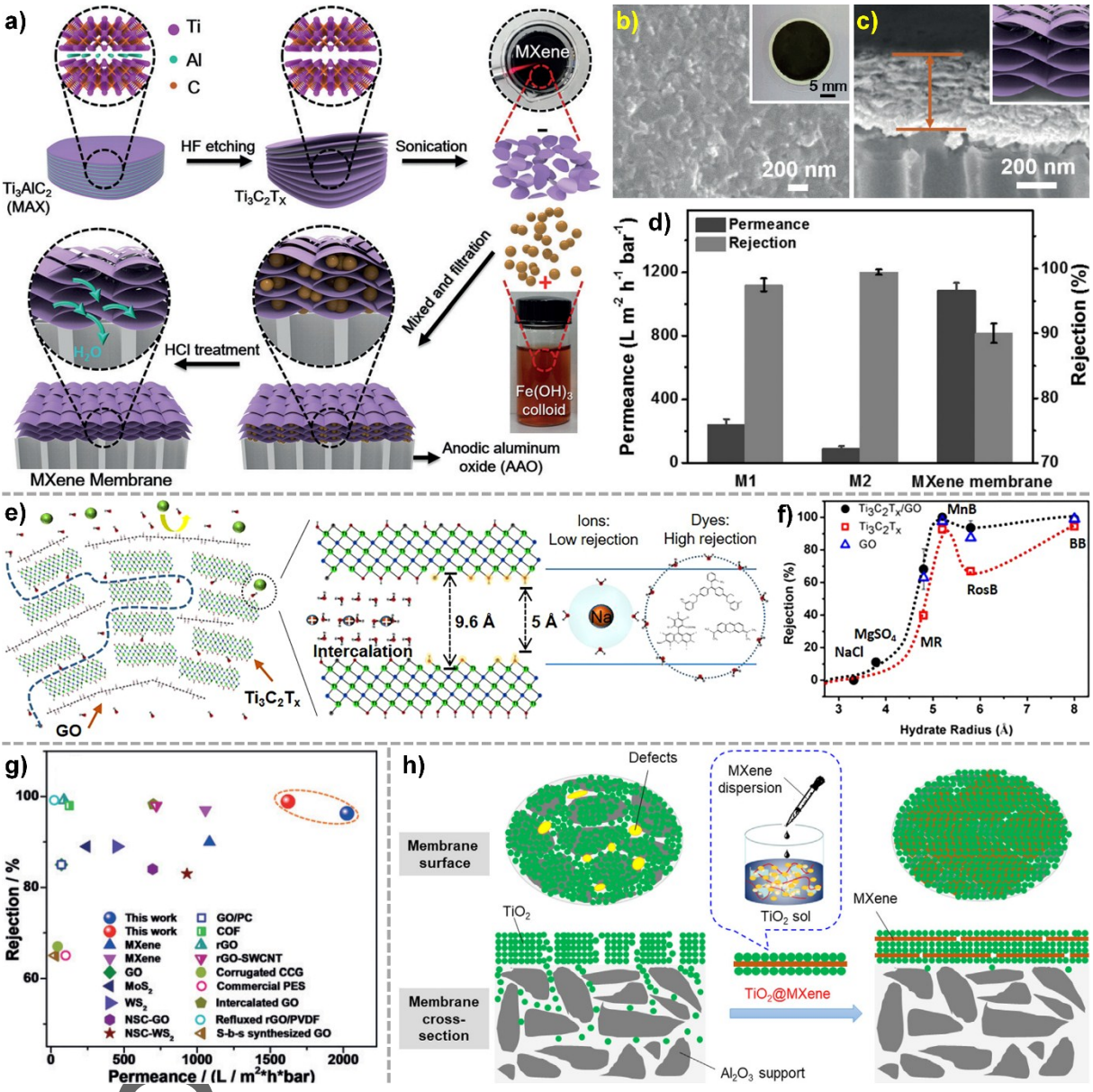

Figure 5. Water purification by MXene-based membranes. (a) Preparation, (b,c) characterization, and (d) performance of MXene-based NLMs with enlarged interlayer spacing achieved by the intercalation and subsequent removal of colloidal $Fe(OH)_3$. (a-d) Reproduced with permission.[71] Copyright 2017, Wiley-VCH. (e) Conceptual diagram of size exclusion by GO-MXene hybrid membrane. (f) Rejection efficiency comparison of GO-MXene hybrid membrane with respect to GO and MXene. (e-f) Reproduced with permission.[94] Copyright 2017, American Chemical Society. (g) Performance comparison of MXene-based membranes and other 2DM-based or commercial polymeric membranes for rejection of various dye molecules. Reproduced with permission.[109] Copyright 2017, Wiley-VCH. (h) Effect of MXene nanosheets on defect prevention in TiO_2 mesoporous membranes. Reproduced with permission.[92] Copyright 2018, Elsevier B.V.

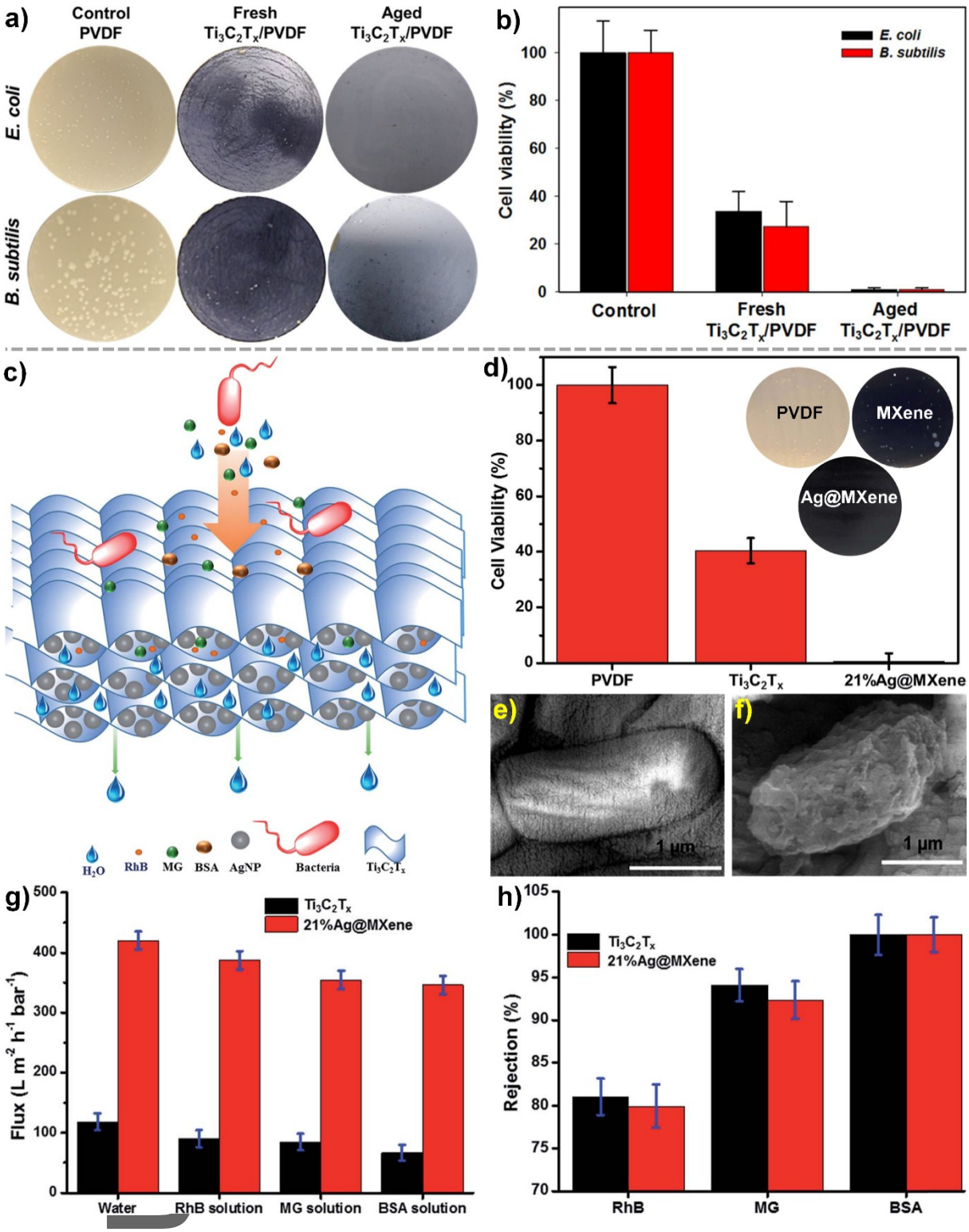

Figure 6. MXene-based antibacterial membranes for water purification. (a) Colonies and (b) viable counts comparison of Gram-negative and -positive bacteria on PVDF support, and MXene membranes. (a,b) Reproduced under the terms of a Creative Commons Attribution 4.0 International License.[85] Copyright 2017, The Authors, published by Springer Nature. (c) Illustration of the hybrid

AgNP-MXene membrane. (d) Survival of bacterial cells exposed to PVDF, MXene, and Ag@MXene membranes. (e,f) Bacterial cells (e) before and (f) after Ag@MXene exposure. (g) Water flux, and (h) solute rejection of MXene and Ag@MXene membranes. (c-h) Reproduced with permission.[86] Copyright 2017, Royal Society of Chemistry.

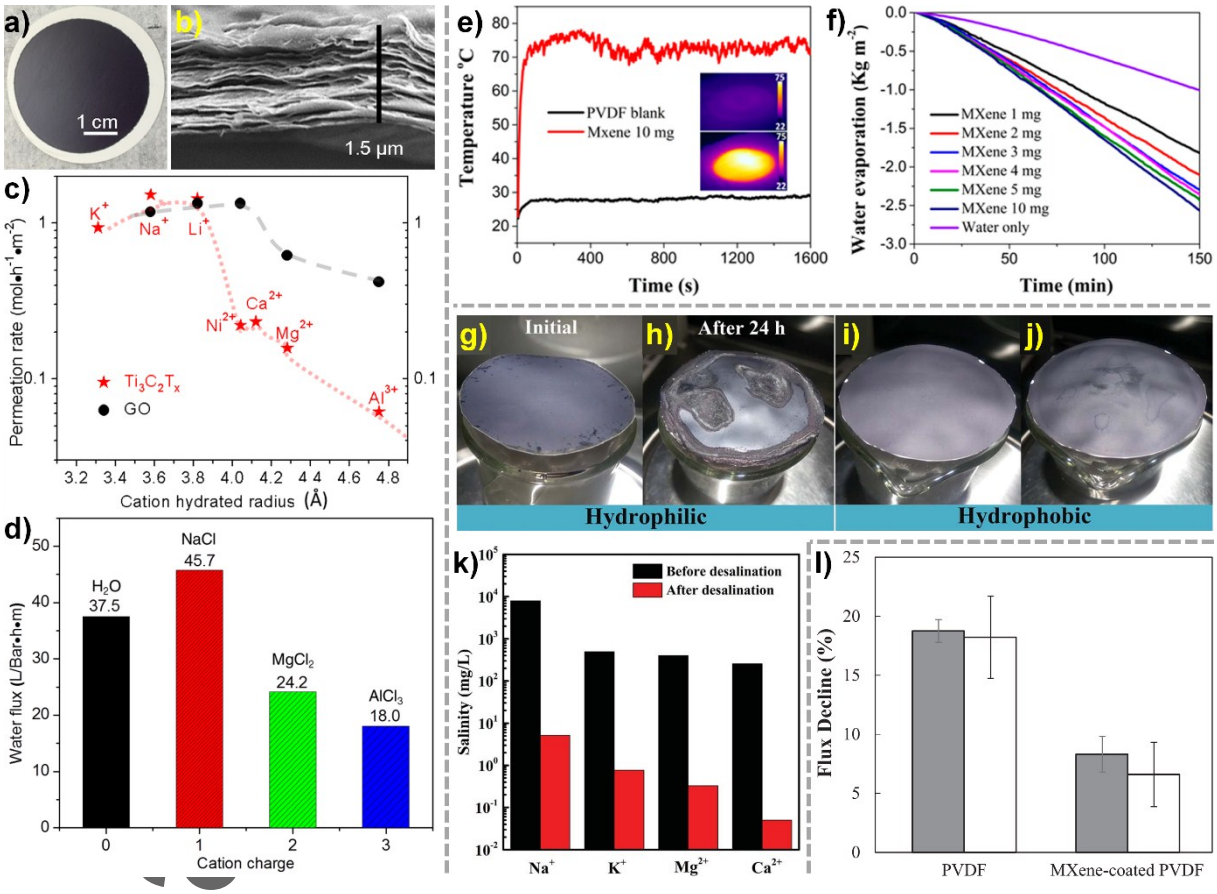

Figure 7. MXene-based membranes developed for desalination applications. (a) Top-wide and (b) magnified cross-sectional views of a nanolaminate MXene ($Ti_3C_2T_x$) membrane for ion sieving. (c) Permeation rates of different cations through MXene and GO nanolaminates membranes. (a-c) Reproduced with permission.[60] Copyright 2015, American Chemical Society. (e) Time-dependent heating profiles of PDMS-modified PVDF and PVDF-supported MXene NLMs under one sun illumination in the open-air atmosphere (inset: membranes under infrared camera). Reproduced with permission.[125] Copyright 2017, American Chemical Society. (g-j) MXene-based (g,h) hydrophilic and (i,j) hydrophobic membranes (g,i) before and (h,j) after 24-h solar desalination. (k) Photothermal desalination performance of MXene-based hydrophobic nanolaminate for different cations. Adapted with permission.[126] Copyright 2018, Royal Society of Chemistry. (l) Flux decline of PVDF and PVDF-supported MXene nanolaminates membranes after a 21-h photothermal membrane distillation with a feed composition of 10 $g \cdot L^{-1}$ NaCl and 200 ppm BSA (as foulant). (g-l) Reproduced with permission.[127] Copyright 2018, Elsevier B.V.

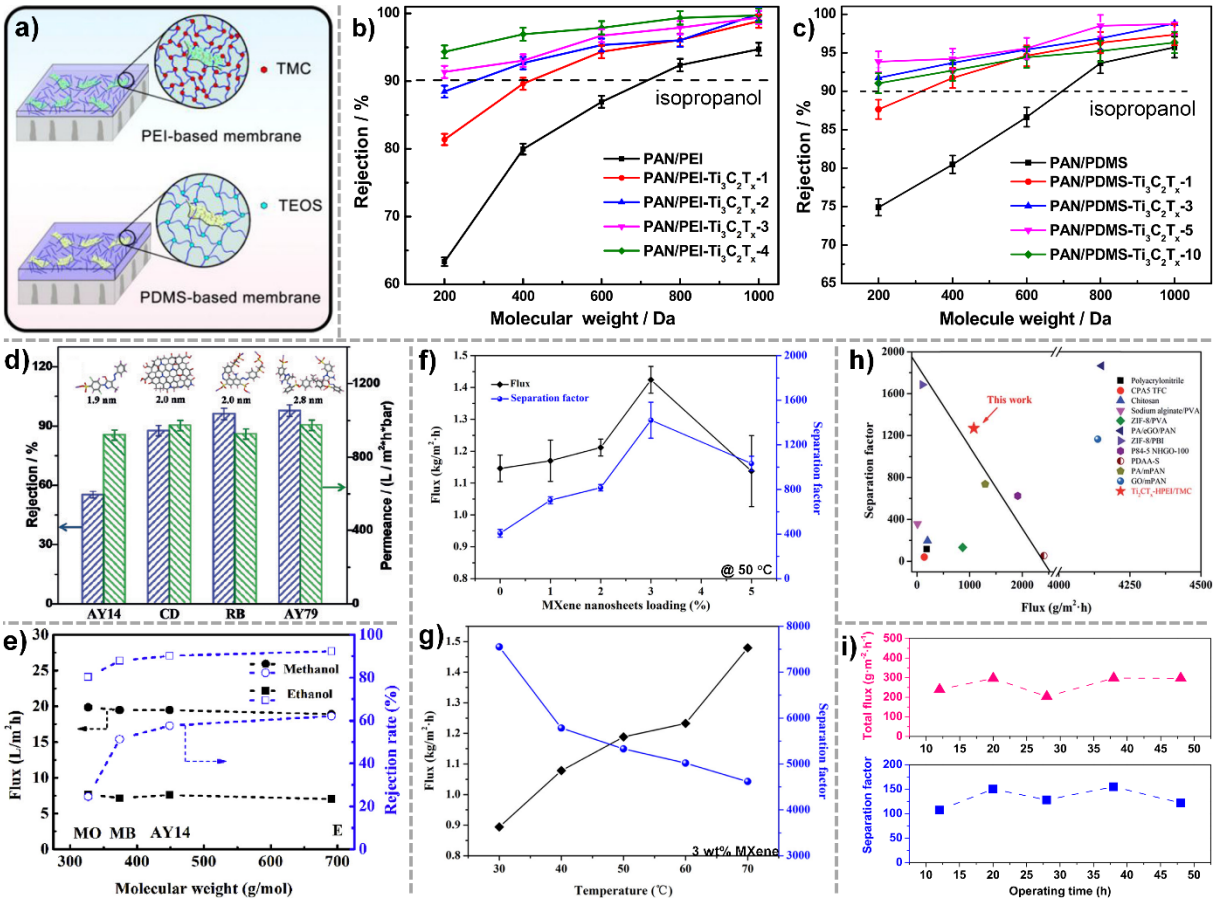

Figure 8. MXene-based membranes developed for solvent purification applications. (a) Schematics of the preparation of MXene-filled TFN membranes prepared by using PAN as support and PEI or PDMS as the selective layer matrix. Reproduced with permission.[79] Copyright 2017, Elsevier B.V. (b,c) PEG rejection performances of (b) PAN/PEI-MXene and (c) PAN/PDMS-MXene membranes from isopropanol. (b-c) Reproduced with permission.[75] Copyright 2016, Elsevier B.V. (d) Removal of different dyes from isopropanol using Nylon-supported MXene nanolaminates. Reproduced with permission.[109] Copyright 2018, Wiley-VCH. (e) Removal of various dyes from methanol and ethanol using GO/MXene nanolaminates (with 70 wt% MXene). Reproduced with permission.[130] Copyright 2019, Elsevier B.V. (f,g) Dehydration of (f) ethanol (10 wt% water) and (g) ethyl acetate (2 wt% water) using chitosan-MXene MMMs. (f,g) Reproduced with permission.[96] Copyright 2018, Elsevier B.V. (h) Performance comparison of PAN/PEI-MXene TFN membrane for the dehydration of isopropanol (90 wt% water). Reproduced with permission.[131] Copyright 2018, Royal Society of Chemistry. (i) Long-term dehydration of ethanol (95 wt%) using MXene nanolaminates at room temperature. Reproduced with permission.[132] Copyright 2019, Elsevier B.V.

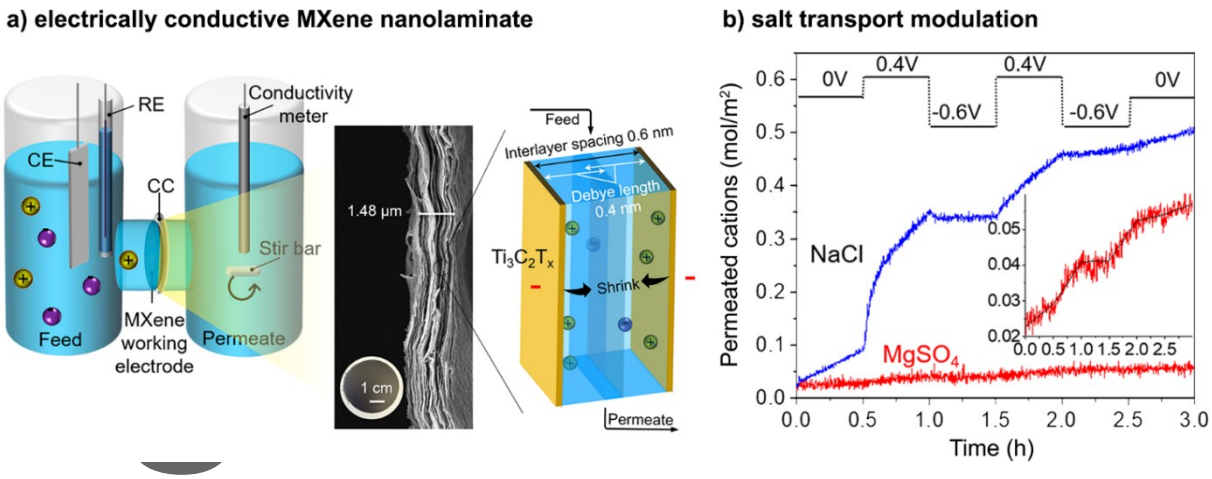

Figure 9. (a) Schematic illustration showing a U-shaped device, where a PVDF-supported MXene ($Ti_3C_2T_x$) membrane was placed in the center as a working electrode with an annular Ti foil as a current collector (CC). (CE and RE stand for counter electrode and reference electrode, respectively.) (b) Salt transport through the MXene membrane can be modulated as exemplified by the ability to control the permeation of cations by tuning the applied voltage. Reproduced with permission.[84] Copyright 2018 American Chemical Society.

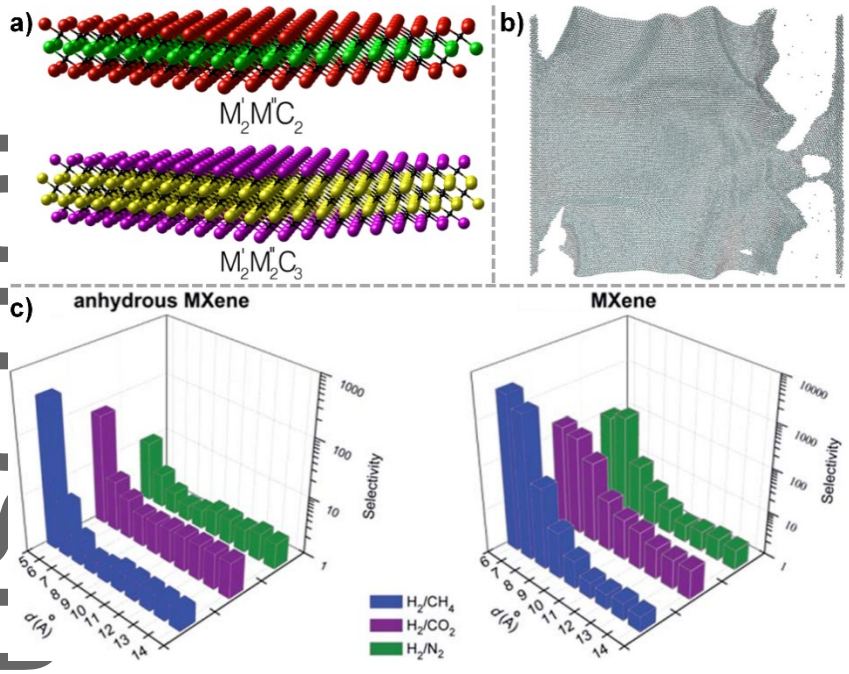

Figure 10. Simulation-aided materials design in MXenes. (a) Double-transition-metal M'M"C_2 and M'M"C_3 MXenes. Reproduced with permission.[170] Copyright 2015, American Chemical Society. (b) Atomistic configuration of the Ti_2C MXene under strain. Reproduced with permission.[172] Copyright 2015, IOP Publishing Ltd. (c) Diffusion selectivity of H_2 with respect to CH_4 (blue), CO_2 (purple), and N_2 (green) for anhydrous MXene and hydrous MXene membranes. Adapted with permission.[173] Copyright 2018, Royal Society of Chemistry.

Biographies

H. Enis Karahan pursued his doctoral studies at the Bioengineering Division of Nanyang Technological University. He holds bachelor's degrees in Chemical Engineering and Molecular Biology and Genetics earned from Istanbul Technical University. He also received a master's degree in Materials Science and Engineering at Koç University. In the Singapore Membrane Technology Centre (postdoctoral fellow) and The University of Sydney (visiting scholar), he focused on polymer-based membrane contactors, nanosheet-based separation membranes, and antibacterial and antibiofouling materials. His research interests include molecular self-assemblies, thin films, surface coatings, carbon-based materials, nanomedicine, and composite membranes.

Kunli Goh received his B.Sc. (Hons) in Chemistry from the National University of Singapore in 2004. He served as a Chemistry Subject Head in a high school in Singapore before returning to pursue his Ph.D. degree in the Sustainable Earth Program by the Interdisciplinary Graduate School of Nanyang Technological University in 2016. He is currently a postdoctoral fellow in Rong Wang's research group at the Singapore Membrane Technology Centre. His research interests focus on the synthesis, functionalization and nanoarchitectonics of advanced functional materirals for developing gas separation and water treatment membranes.

Tae-Hyun Bae received his B.Sc., M.Sc., and Ph.D. degrees from the School of Biological Resources and Materials Engineering of Seoul National University. He earned his second Ph.D. in Chemical Engineering at Georgia Institute of Technology in 2010. Following a postdoctoral experience at the University of California, Berkeley, he had served as an Assitant Professor at Nanyang Technological University, Singapore, from 2013 to 2019. Since 2019, he has been working as an Associate Professor of Chemical Engineering at KAIST.

This Review pinpoints the current status and future potential of MXene-based separation membranes. After providing a basis on MXene synthesis and membrane design, separation applications of MXene-based membranes are introduced, namely gas separation, water treatment (e.g., solute removals and bacterial disinfection), desalination, and organic solvent purification. As future perspectives, polymer nanocomposites, electroresponsive/reactive membranes and simulation-driven membrane design are discussed.

Keyword 2D nanomaterial; Titanium carbide; Nanocomposite; Nanolaminate; Coating

H. E. Karahan, K. Goh, C. J. Zhang, E. Yang, C. Yıldırım, C. Y. Chuah, M. G. Ahunbay, J. Lee, Ş. B. Tantekin-Ersolmaz, Y. Chen, T.-H. Bae*

Title MXene Materials for Designing Advanced Separation Membranes